OIL RETENTION AND PRESSURE DROP IN HORIZONTAL AND VERTICAL SUCTION LINES WITH R410A / POE ISO 32

BY

KURT F. ZOELLICK

THESIS

Submitted in partial fulfillment of the requirements
for the degree of Master of Science in Mechanical Engineering
in the Graduate College of the
University of Illinois at Urbana-Champaign, 2010

Urbana, Illinois

Adviser:

Professor Predrag S. Hrnjak

ABSTRACT

In refrigeration systems a small amount of compressor lubricant is entrained in the refrigerant and circulated through the system, where some is retained in each component. The suction line to the compressor has the largest potential for oil retention. This paper presents results from an experimental apparatus that has been constructed to circulate POE (polyolester) oil and R410A at a controlled mass flux, OCR (oil in circulation ratio), and apparent superheat, and to directly measure the pressure drop and mass of oil retained in horizontal and vertical suction lines. The bulk vapor velocity and overall void fraction are determined from direct mass and temperature measurements. The oil retention, pressure drop, and flow regimes near the minimum ASHRAE recommended mass flux condition are explored. It was found that oil retention begins to increase sharply even above the minimum recommended flux, so conditions near the minimum should be avoided. Two relationships were developed to predict the oil retention in the vertical and horizontal suction lines. The average error from the predictions method was 10.9% for the vertical tube, and 7.9% for the horizontal tube.

To My Father and Mother

ACKNOWLEDGEMENT

I would like to thank Ankit Sethi for his help in completing experiments for this project, and editing this paper. I would like to thank Scott Wujek and Augusto Zimmerman for your advice, support, and editing of this paper. I would like to thank my advisor, Pega Hrnjak for his support throughout this project. I would also like to give a special thanks to the members of the Air Conditioning and Refrigeration Center at the University of Illinois for their support.

TABLE OF CONTENTS

NOMENCLATURE

Symbol	Meaning	Units
A(w_{local})	Empirical expression	
a_{0-4}	Empirical coefficients	
B(w_{local})	Empirical expression	
b_{0-4}	Empirical coefficients	
D	Pipe diameter	(m)
δ	Average film thickness	(m)
δ_o	Corrected film thickness	(m)
f_i	Interfacial friction factor	
G	Mass Flux	(kg/m^{2}s)
g	Gravitational acceleration	(m/s^2)
j^*_g	Normalized vapor velocity	(m/s)
m_r	Refrigerant tank mass flow	(g/s)
m_{o_tank}	Oil tank mass flow	(g/s)
ν_l	Liquid kinematic viscosity	(Pa·s)
ν_v	Vapor kinematic viscosity	(Pa·s)
OCR	Oil in circulation ratio	
P_{sat}	Saturation pressure	(MPa)
ρ_l	Liquid density	(kg/m^3)
ρ_v	Vapor density	(kg/m^3)
ρ_{mix}	Mixture density	(kg/m^3)
ρ_o	Oil density	(kg/m^3)
ρ_r	Refrigerant density	(kg/m^3)
q	Liquid volume flow rate / πD	(m^2/s)
Re_l	Liquid Reynolds number	
τ_i	Interfacial shear stress (l-v)	(N/m^2)
T_{bub}	Bubble temperature	(C)
T_{o_tank}	Oil tank temperature	(C)
ΔT_{sh}	Apparent superheat	(C)
u_v	Superficial vapor velocity	
w_{local}	Mass fraction oil in liquid phase	
w_{o_tank}	Mass fraction of oil in oil tank	

1 INTRODUCTION

The oil holdup in components of a refrigeration system has been the focus of many studies over the last 40 years. The suction line of a refrigeration system, especially for large commercial or building systems, can be a major location of oil holdup. The low temperature and high quality inside of a suction line means the small amount of liquid will be very oil rich and have a high viscosity. A high velocity of refrigerant vapor is required to pull the oil through long suction lines, especially in vertical, upwards flow conditions. The demand for energy efficient A/C systems has pushed many innovations, such as variable speed compressors, to reduce power usage during low load conditions. Oil retention can especially be a problem during low-load conditions due to lower vapor velocities in the suction line. These problems are alleviated by the use of parallel risers and u-traps, but both of these solutions increase piping expense, increase pressured drop, and still may not completely solve oil return problems. A better understanding of suction line flow regimes and oil retention during low velocity conditions is necessary for development of better suction risers.

Van Rossum (1959) conducted one of the first few studies into liquid films. He measured the thickness of films on a flat surface with a controlled flow rate of vapor above. He was able to correlate the thickness of the liquid film to the liquid Reynolds number, using a force balance on the film. His dimensionless parameters were used in the current study to relate film thickness.

In 1968, Marc Jacobs published the first, and still most influential, paper about oil return in suction risers. His experiment simulated the suction line of a refrigeration system by injecting oil at the bottom of a vertical pipe with sight glasses to monitor flow regimes. He decreased the refrigerant flow rates until he saw “flooding” in the sight glass, a churn/slug flow regime, which develops at the bottom of the tube as oil accumulates. He used visualization data to develop equation 1.1, to predict the minimum mass flux for sufficient oil return. (Jacobs *et. al.* 1968)

$$G = \left(j_g^{*\frac{1}{2}}\right)^2 [\rho_v g D(\rho_l - \rho_v)]^{0.5} \tag{1.1}$$

$$j_g^{*\frac{1}{2}} = 0.85 \ \ (empirically\ determined\ for\ R12\ and\ 150\ SUS\ oil)$$
$$\rho_v = vapor\ density$$
$$\rho_l = liquid\ density$$
$$D = Pipe\ Diameter$$
$$g = Acceleration\ due\ to\ Gravity$$

The dimensionless j* relates momentum flux of the vapor to the gravitational and buoyant forces. The value of 0.85 was empirically determined from the visualization experiments. This relationship is used in the ASHRAE refrigeration handbook as the basis for suction riser sizing. The equation provides a simple solution to sizing suction risers, but omits factors such viscosity effects. In a real system, oil will be returned at any flow condition as long as there is enough oil charge to satisfy the oil retention demands of the system components.

Some recent oil return studies have been completed at University of Maryland in Professor Reinhard Radermacher’s group. Radermacher *et. al.* (2006) presented a method of calculating oil retention in suction lines based on a physical model of the liquid film and data from his students. There is some discrepancy with measured values, which may be due to the differing methods of oil injection used. Lee *et. al.* (2001) measured oil retention with the injection-separation method in the suction line of a freezer system that used both R134a /

alkylbenzene oil mixture and R134a / mineral oil mixture. The flow regimes were annular and churn depending on the vapor flux, and their model predicted oil retention within 25% of the measured values.

Mehendale and Radermacher (2000) experimented with vertical upward flows of refrigerant and oil in a suction line. Using visualization techniques similar to Jacobs, they determined at which conditions the liquid annulus began to reverse the direction of the flow and start to move downwards. They referred to this point of flow reversal as the “critical velocity.” Their experiments determined this critical velocity for some mixtures, and a physical model for determining the critical velocity was developed based on their findings and previous interfacial friction factor relationships from Wallis (1969).

Cremaschi *et. al.* (2005) continued the experiments using the same facilities as Mehendale. Measurements of oil retention were taken in the suction line as well as other system components. The injection-separation method was used, where oil was injected at the bottom of a pure refrigerant suction line and separated out at the top of the suction line. The time between the injection and separation was measured to determine the liquid velocity and retention rate. One downside to this method was that the injection of oil generates a non-equilibrium condition inside of the suction riser, because some refrigerant may be dissolving into the oil during the test. In addition, injection of oil into the vertical pipe does not simulate the entrance condition to a real system, where oil may be able to accumulate in the bottom. Cremaschi discussed trends for oil retention with changing OCR, mass flux, oil viscosity, and pipe diameter, and worked with Radermacher *et. al.* (2006) to develop the physical model for the oil annulus in a suction line.

Research involving refrigerant oil was also being conducted at the Air Conditioning and Refrigeration Center at the University of Illinois. Crompton *et. al.* (2004) studied oil retention in horizontal smooth and finned tubes with various refrigerant and oil mixtures. While the system is running at equilibrium, valves on both ends of the test section were closed simultaneously, and the test section was then removed and weighed. The refrigerant was then removed, and the test section was weighed again to determine the mass of oil retained. This method gave very accurate results via a direct measurement of oil retention. They developed a model for predicting oil retention in horizontal pipes for conditions with two-phase refrigerant.

Other researchers studied oil retention at the University of Illinois. Sheth and Newell (2005) studied oil migration in an air conditioning system. Jassim and Newell (2005) investigated the void fraction with oil and refrigerant flows in tubes with the use of a probabilistic flow regime map. Burr *et. al*. (2005) studied oil retention and two phase flow in microchannels. They clamped the ends of the microchannels during steady state flow conditions in order to measure the retention and void fraction.

2 EXPERIMENT SYSTEM

An experimental facility was constructed to circulate refrigerant and oil at controlled flow rates and thermodynamic states, to simulate the suction line of a typical R410A A/C system. A schematic of the system can be seen in Figure 2.1. The fluids used in the test are R410A and nominally 32 cSt POE oil. The setup had one vertical, with upward flow, and one horizontal test section made of clear PVC tubes, each of which was about 2 m long. There were valves on both sides of the test sections, which were closed simultaneously during steady state conditions to measure the mass of oil retained inside of the test sections. There were pressure taps at both ends of the test sections, which allowed for pressure drop measurements.

A helical liquid separator at the exit of the vertical test section separated the vapor and liquid. The liquid, which was a mixture of oil and dissolved refrigerant, flowed into the oil tank. The vapor flowed into a 12-plate condenser, where it was completely condensed into liquid. The condenser operated in a counter-flow orientation with the cooling fluid being chilled water at around 6 °C. The condensed refrigerant flowed into a receiver made from a 2” inner diameter copper tube and then into a subcooler. The refrigerant was then pumped through by a gear pump controlled with a variable frequency drive. The flow rate and density of the refrigerant liquid was measured with a MicroMotion CMF25 Coriolis flow meter. The accuracy and repeatability of the mass flow measurements are ±0.1% and ±0.05% of the flow rate, respectively. The accuracy of the CMF25 density measurement is ±0.5 kg/m^3 and the density was checked against known values in the Engineering Equation Solver to ensure that the refrigerant was pure.

The oil, with some dissolved refrigerant, was pumped from the oil tank and through a subcooler by another gear pump. The oil pump was driven by a fixed frequency AC motor, and the flow rate was controlled with a bypass valve. A MicroMotion CMF10 Coriolis flow meter measured the flow rate and density of the oil rich liquid before it was mixed with the pure refrigerant stream. The accuracy and repeatability of the mass flow measurements are ±0.1% and ±0.05% of the flow rate reading respectively. The accuracy of the density measurement is ±0.5 kg/m^3. A T-type thermocouple (±0.5 °C) measured the temperature of the oil flow at the entrance to the flow meter. The concentration of refrigerant dissolved in the oil flow was calculated from the temperature and density of the oil mixture as described in the next section. The OCR at the inlet of the test section was controlled by adjusting the flow rate of the pure refrigerant stream and the oil stream. A typical OCR measurement with associated uncertainty would be 0.03 ± 0.0008.

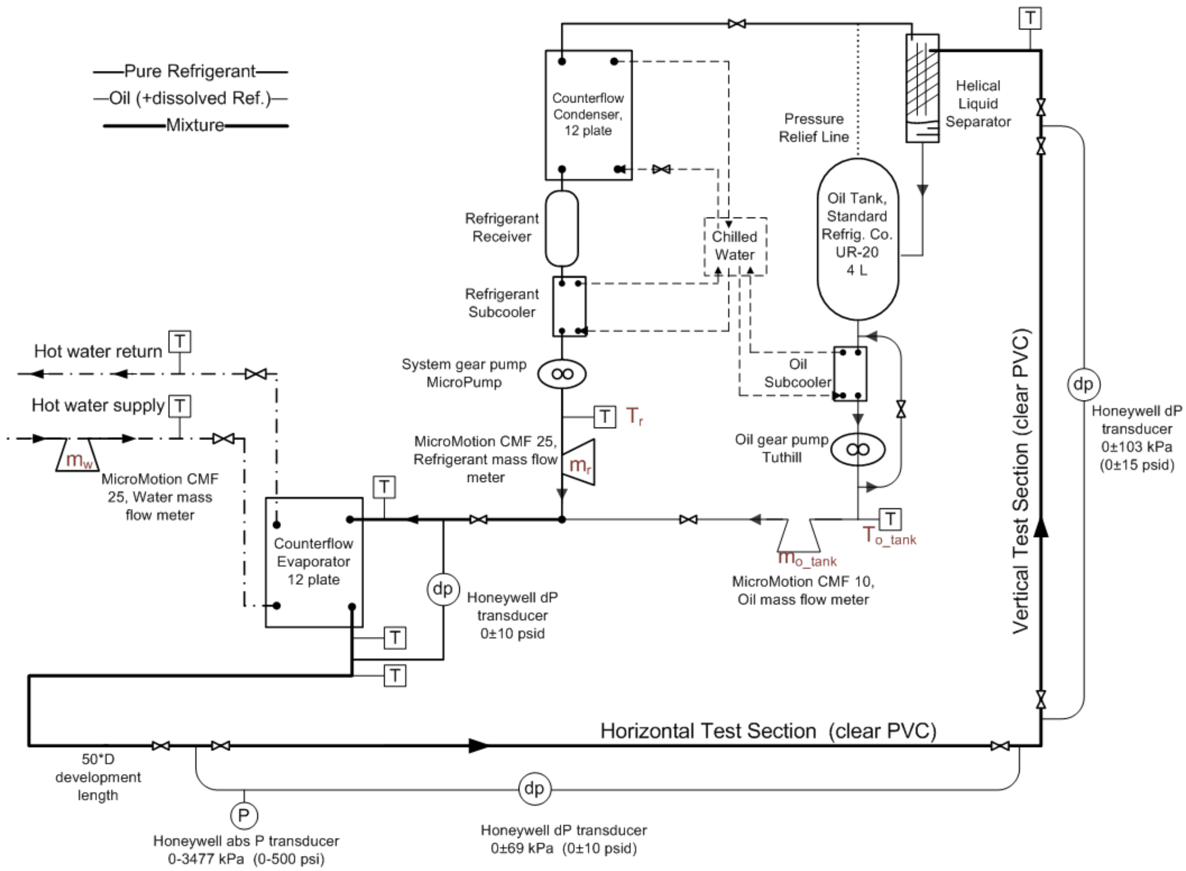

Figure 2-1 Schematic drawing of the facility

The refrigerant and oil streams were mixed and flowed into a 12 plate counter-flow evaporator. The flow rate and temperature of the hot water in the evaporator were controlled, so the refrigerant and oil mixture could be held at the desired apparent superheat. The temperature of the water was typically set at or slightly above the desired apparent superheat, and a high water flow rate was used. The temperature of the refrigerant at the evaporator outlet was measured in the center of the tube and on the outside of the tube wall underneath the insulation, in order to ensure that the two phases were in thermal equilibrium. In addition, a 50 diameter long development length was placed before the horizontal test section inlet, to ensure thermal and hydrodynamic flow development. The concentration of oil in the liquid phase was dependent on the temperature and saturation pressure of the flow, both of which remained within ±3% or ±1 °C of the set value during a test.

Mixing the refrigerant and oil in the liquid phase before the evaporator emulated a real system and ensured that the liquid and vapor were very near equilibrium at the inlet of the test section. We believe this method was more realistic than injection of oil alone into the vertical pipe with pure refrigerant vapor flowing upwards. When pure oil is directly injected into the suction pipe, the liquid phase may not be in equilibrium with the vapor, affecting the density, viscosity, and other important properties of the liquid film. When the oil is mixed with refrigerant before the evaporated, the liquid film remains in equilibrium with the vapor in the tube.

The inlet to the vertical test section was a standard 90° elbow fitting with the same inner diameter as the test sections. It is important to note that the use of a standard elbow might have some unknown effect on the flow regimes in the vertical test section. The effect of using a long radius elbow or a p-trap at the inlet to the vertical test section was not examined. There are no experimental results or correlations in the literature for the entrance condition to the vertical pipe. While many companies recommend the use of p-traps at the exit of the evaporator, real systems do not use p-traps at every horizontal to vertical elbow. Therefore the results from these experiments should be applied with caution when p-traps are used.

The saturation pressure was measured at the inlet to the horizontal test section by a Honeywell TJE absolute pressure transducer, with a range 0 to 3477 kPa and accuracy ± 8.6 kPa. The pressure drop across the horizontal test section was measured with a Honeywell Z differential pressure transducer, having a range 0 ± 69 kPa and accuracy ± 0.1 kPa. The pressure drop across the vertical test section was measured with a Honeywell Z differential pressure transducer, with a range 0 ± 103 kPa and accuracy ± 0.26 kPa.

Outputs from all thermocouples, pressure transducers, and Coriolis flow meters are read by a Yokogawa HR1300 data-logger. The data-logger interfaces with a computer running a LabView program to display and record all measured data. Important parameters, such as OCR from the flow rate, density, and temperature, are displayed in real time.

3 TESTING PROCEDURE

3.1 OCR and Local Oil Concentration Measurements:

A gear pump pumped the liquid from the pure refrigerant tank through a MicroMotion CMF25 coriolis mass flow meter. The mass flow meter measured the flow rate of the liquid refrigerant (m_r). The temperature at the inlet to the CMF25 was measured with a thermocouple (T_r).

A separate gear pump was used to pump the saturated refrigerant-oil mixture from the oil tank, through a MicroMotion CMF10 coriolis mass flow meter, and into the mixing section. The mass flow rate (m_{o_tank}) and density (ρ_{o_tank}) of the oil mixture in the oil tank were measured by the CMF10. A thermocouple at the inlet to the CMF10 measured the temperature of the oil mixture (T_{o_tank}), and the saturation pressure was measured in the test section. The concentration of oil in oil tank (w_{o_tank}) was determined from the density, pressure, and temperature measurements using equations 3.1 through 3.3 below.

$$w_{o\_tank} = \left[\frac{\rho_o}{\rho_{o\_tank}(\rho_r - \rho_{o\_tank})}\right] / (\rho_r - \rho_o) \tag{3.1}$$

$$\rho_r = -0.02054 * T_{o\ tank}{}^2 - 4.08654 * T_{o\ tank} + 1176.67 \quad (T_{o\_tank} \text{ in °C}) \tag{3.2}$$

$$\rho_o = -0.0004342 * T_{o\ tank}{}^2 - 0.58704 * T_{o\ tank} + 984.91 \quad (T_{o\_tank} \text{ in °C}) \tag{3.3}$$

Equation (3.1) is the ideal mixing equation applied for the mixture of refrigerant and oil. Density and viscosity data for R410A and POE ISO 32 mixed acid oil were taken from Cavestri & Schafer (2000), whose figures are used in the ASHRAE Refrigeration Handbook (2002).

Equations (3.2) and (3.3) are quadratic equations fit to the density and temperature of the pure oil (ρ_o) and pure refrigerant (ρ_r). Equation (3.2) was found using the embedded refrigerant property data from the Engineering Equation Solver program, and the curve fit function in Microsoft Excel. Equation (3.3) is also a curve fit from Microsoft Excel, for the density of the oil taken from Chapter 7 of the 2002 ASHRAE Handbook. The flow rate of pure oil is equal to the total flow rate out of the oil tank (m_o) multiplied by the concentration of oil in the oil tank (w_{o_tank}). The OCR is the ratio of the mass of pure oil to the total mass of oil and refrigerant. The measurement of mass flow rates of the two streams makes this calculation relatively simple, as shown in equation (3.4)

$$OCR = \frac{(m_{o\_tank} * w_{o\_tank})}{(m_{o\ tank} + m_r)} \tag{3.4}$$

The two liquid streams were mixed in a tee connection, and entered the evaporator. The evaporator was a plate heat exchanger which was oriented such that the refrigerant and oil flowed downwards through it. This was done to reduce the oil retention in the evaporator. The temperature and flow rate of water from a secondary system were adjusted such that the refrigerant mixture exited at an intended apparent superheat. The apparent superheat is defined here as the difference between the temperature of the mixture measured on the tube wall and the saturation temperature of pure refrigerant at the pressure measured at the inlet to the test section. The overall quality and local oil concentration in the liquid could be determined from the pressure and temperature measurement, using the method for R22 and AB oil presented by Takaishi & Oguchi (1987), and later expanded to other refrigerants and oils by Thome (1995).

The empirical equation for determining bubble point temperature (temperature of the liquid) for a given saturation pressure and local oil concentration in the liquid is shown in equation (3.5).

$$T_{bub} = \frac{A(w_{local})}{\ln(P_{sat}) - B(w_{local})} \tag{3.5}$$

In equation (3.5) T_{bub} is the bubble point temperature in K, P_{sat} is the saturation pressure of the mixture in MPa, and A and B are empirically determined expressions for certain oil and refrigerant mixtures.

$$A(w_{local}) = a_0 + a_1 w_{local} + a_2 w_{local}^3 + a_3 w_{local}^5 + a_4 w_{local}^7 \tag{3.6}$$

$$B(w_{local}) = b_0 + b_1 w_{local} + b_2 w_{local}^3 + b_3 w_{local}^5 + b_4 w_{local}^7 \tag{3.7}$$

a_0 = -2363.0	b_0 = 8.427
a_1 = 182.52	b_1 = -0.72212
a_2 = -724.21	b_2 = 2.3914
a_3 = 3868.0	b_3 = -13.779
a_4 = -5268.9	b_4 = 17.066

The equations must first be adjusted to the refrigerant that is being used. This is done by setting w_{local} to zero, and calculating a_0 and b_0 using two sets of known saturation pressure and temperature values for the pure refrigerant. This was done for R410A in this experiment, and the values found are shown above. The vapor pressure of oil is extremely small compared to the refrigerant, and therefore the type of oil used has a small effect on the empirical constants a_1 through a_4 and b_1 through b_4 for oil concentrations up to 70% (Thome, 1995). The constants a_0 and b_0 should be reevaluated for any change in saturation pressure of the system.

Equation (3.5) has three unknowns: saturation pressure, bubble temperature, and local concentration. A program in Engineering Equation Solver was written to calculate the local concentration of oil in the liquid at known saturation pressure and bubble temperature, both of which were measured at the inlet to the test section. The local quality can be determined from equation (3.8). Note that the maximum quality is (1-OCR) since the oil will always remain in the liquid phase.

$$w_{local} = OCR/(1-x) \tag{3.8}$$

This quality is the ratio of the mass flow rate of liquid to the total mass flow rate entering the test sections at steady state conditions. It is not equal to the mass ratio of liquid and vapor inside of the tube at any given time. This is because some extra liquid is retained inside of the suction line.

3.2 Oil Mass Retention Measurements:

The system was adjusted to the desired test conditions: flow rate, OCR, and apparent superheat. The flow rate and OCR were adjusted by controlling the refrigerant pump speed and oil bypass valve opening. When running, during the transient period, the pressure drops across the test sections were monitored. Once both pressure drop measurements maintained a steady value, the system was allowed to run for at least 5 additional minutes, to assure steady state operation. Data from all sensors was then recorded for the next 5 minutes. If any recorded conditions varied by more than 3% or 1 °C during this period, the test run was discarded and the condition was re-run. Once the data was collected, the valves on either side of the test section were shut simultaneously, and the test sections were removed for weighing.

The test sections were removed from the system and the exterior was cleaned to remove any particles or oil. The tubes were then weighed on an electronic balance and the weight was compared to that of the empty tubes. The accuracy of the balance was ±0.03 g. This measurement represents the total amount of refrigerant and oil inside of the tube. The tube was then placed vertically and refrigerant vapor was slowly removed from the top of the tube until no bubbles could be seen coming out of the liquid oil under vacuum. The procedure for venting the tube followed ASHRAE standard 41.4. Once the refrigerant was removed from the test section, the test section was again weighed, to determine the mass of oil in the test section. The error of the oil measurement was ±0.06 g, typically about 0.5% of the reading.

A program was developed to predict the oil retention in the suction line based on an overall mass measurement of the test section. The total mass of refrigerant and oil in each test section was obtained from the first mass measurement taken. The local concentration of oil in the liquid could be estimated from equation (3.7), and then the density of the liquid could be estimated. The density of the vapor was known from the temperature and pressure. The internal volume of the test section was calculated from length and diameter measurements of the tube. From this information the mass of oil could be calculated in the test section. Using this technique to avoid venting out the refrigerant can save a significant amount of time for each test. The refrigerant was vented and the actual mass of oil was measured in every test anyway, and the program was able to predict the mass of pure oil within 8% error consistently. Figure 3.1 shows the predicted oil mass versus the measured oil mass for the data points taken in this study.

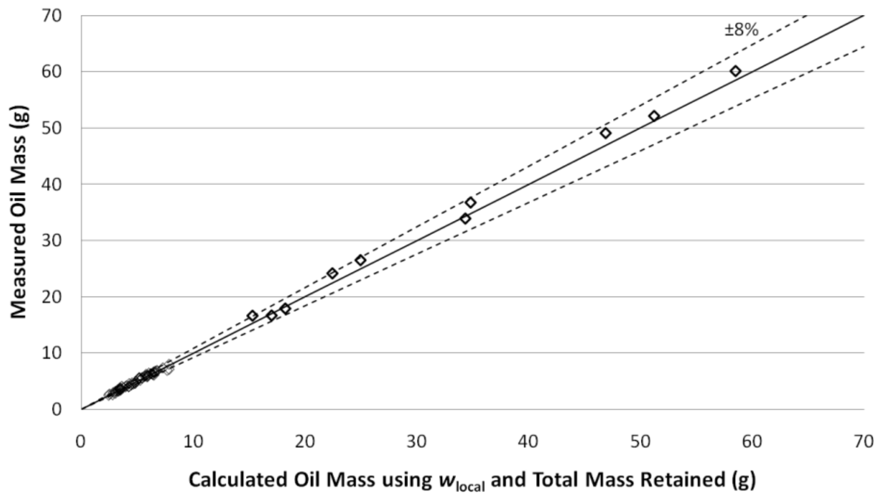

Figure 3-1 Accuracy of Local Concentration Model

The data points shown in Figure 3.1 come from 7.1 mm and 18.5 mm tubes, OCRs of 1%, 3%, and 5%, and apparent superheats of 5 °C, 10 °C, and 15 °C. All but three data points were taken at a saturation pressure of about 1150 kPa (corresponding to a saturation temperature of 12 °C). The pressure drifted up slightly for the high mass flux tests in the 18.5 mm tube, but this has no significant effect on oil retention predictions or measurements. These results show that Takaishi & Oguchi's (1987) method of predicting the local concentration of oil in the liquid refrigerant is accurate within 8% even for 15 °C apparent superheat, where the local oil concentration in the liquid is 75%.

4 RESULTS AND DISCUSSION

4.1 Test Conditions:

Two different pipe diameters, 7.2 mm and 18.5 mm, were studied with three OCRs, 1%, 3%, and 5%, and three apparent superheats, 5 °C, 10 °C, and 15 °C. The range of mass fluxes tested in each pipe is shown in Table 4-1. The minimum recommended mass flux from the Jacobs correlation was 42.9 kg/m^{2}s in the 7.2 mm pipe, and 59.8 kg/m^{2}s in the 18.5 mm pipe. The tests run with the 7.2 mm pipe were all above the minimum mass flux recommended by the Jacobs correlation, due to the minimum flow rate restriction of the system. The larger, 18.5 mm, pipe was used for testing a range of mass fluxes above and below the Jacobs minimum recommended mass flux of 60 kg/m^{2}s. High-speed videos of the flow regimes inside the clear pipes were recorded, and snapshots from these videos are presented in Figures 4-1 through 4-5.

Table 4-1 Mass flux test conditions for each pipe diameter

D=7.2 mm		D=18.5 mm	
Vapor Velocity [m/s]	Mass Flux [kg/m^{2}s]	Vapor Velocity [m/s]	Mass Flux [kg/m^{2}s]
2.8	100	1.6	60
4	150	1.8	70
5	200	2	80
6.5	250	2.8	100

4.2 Horizontal Tube Visualization:

Figure 4-1 and 4-2 present visualization data for the horizontal tube with two different OCRs, Figure 4-1 is for 5% OCR and Figure 4-2 for 1% OCR. The graphs are arranged with apparent superheat on the abscissa and mass flux on the ordinate to correspond with typical flow regime maps. The test section inlet apparent superheat values of 0, 5, 10, and 15 °C correspond to inlet qualities of 0.85, 0.915, 0.928, and 0.935 respectively, which were calculated using the methods explained in Section 3. The difference between the low apparent superheat columns is more noticeable than the difference between the high apparent superheat columns because the quality does not change much once the apparent superheat is above 5 °C.

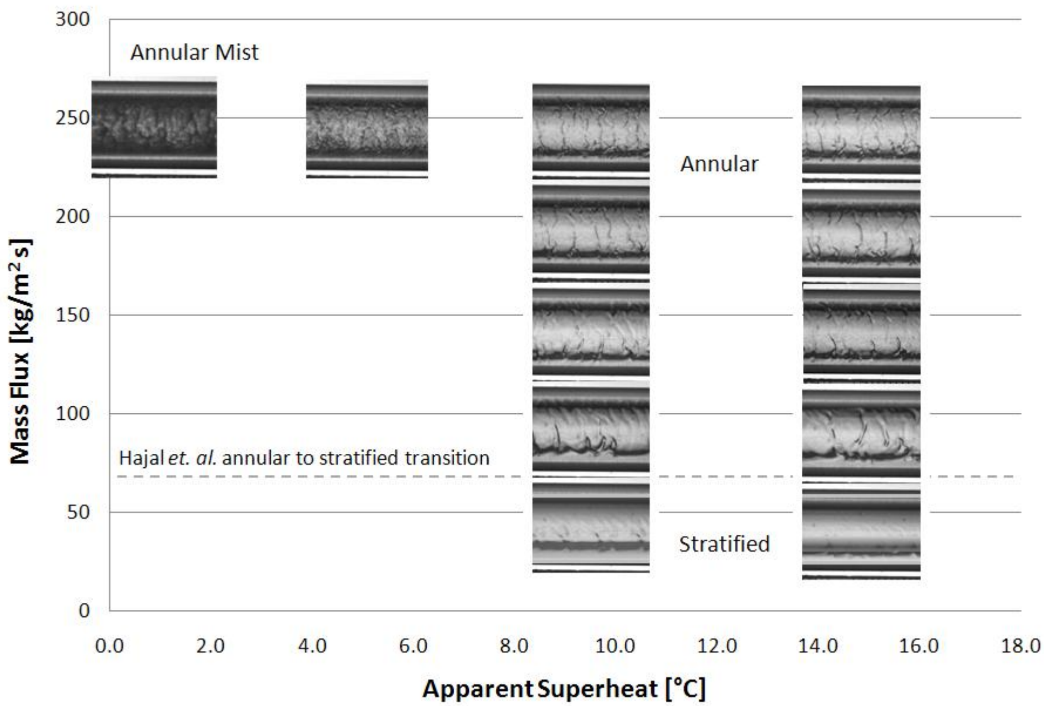

Figure 4-1 Visualization of horizontal tube with 5% OCR

The effect of mass flux can be seen by comparing all of the pictures in a single vertical column. The bottom picture shows a mass flux of 50 kg/m^{2}s, and the liquid forms a smooth stratified layer on the bottom of the tube. As the mass flux is increases, waves appear on the surface of the liquid layer, and the vapor begins to push some of the liquid up onto the walls. This can be seen in the pictures at 100 and 150 kg/m^{2}s. At the highest mass fluxes, the flow regime transitions to annular flow, and a liquid film can be seen covering the entire inner tube surface.

The effect of OCR on the flow regime can be seen by comparing corresponding frames between the Figures 4-1 and 4-2. At high mass flux and high apparent superheat, the film is rippled and completely annular, and OCR has little noticeable effect. As the mass flux decreases and the flow transitions to stratified wavy flow, the effect of OCR is more noticeable in the thickness of the liquid layer and the size of the waves. At low apparent superheat, the increase in the amount of oil causes more bubbles and droplets to form, which allows less light to pass through the test section. This gives the test section a darker and more opaque appearance.

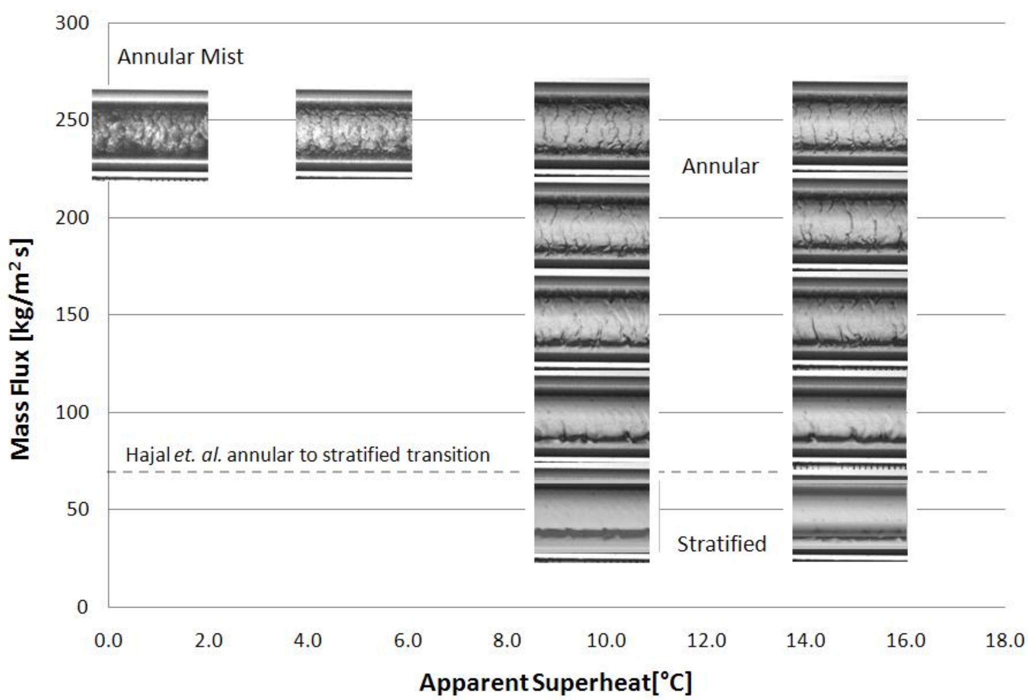

Figure 4-2 Visualization of horizontal tube with 1% OCR

Refrigerant concentration in the liquid phase increases when the apparent superheat at the exit of the evaporator decreases. This causes the properties of the liquid mixture to change; more bubbles and droplets can be seen in the test section at low apparent superheat. As the apparent superheat is reduced to 5 °C, the increased amount of bubbles and droplets allows less light through. If the apparent superheat is allowed to drop to zero, the tube fills with bubbles and droplets as shown in the upper left pictures of Figures 4-1 and 4-2. Since the vapor core is moving much faster than the liquid film, any droplets or bubbles in the core will be transported much more quickly than liquid on the walls.

The flow map from Hajal *et. al.* (2003) predicts that the transition line between annular and stratified flow becomes nearly horizontal at high qualities without heat transfer. The transition line was calculated and is shown on Figures 4-1 and 4-2, and generally agrees with the flow regimes shown. The Hajal flow map was generated for conditions with no oil, however it predicts conditions with oil relatively well when the correct densities and viscosities are used. At high apparent superheats and the mass flux range, the equation in Hajal *et. al.* (2003) seems to be accurate for determining the flow regime. However at low apparent superheats, as shown in Figures 4-1 and 4-2, an annular mist flow is present. This flow structure would not be present in conditions without oil, therefore it not predicted by the Hajal flow map.

4.3 Vertical Tube Visualization:

Figures 4-3 and 4-4 present the visualization data for the vertical transparent test section over the range of conditions tested. Figure 4-3 is for 5% OCR and Figure 4-4 is for 1% OCR. The charts are arranged in the same manner as the horizontal visualization figures, with apparent superheat on the abscissa and mass flux on the ordinate. The apparent superheat is once again analogous to the quality at the inlet to the test sections. It is important to note that the quality at the inlet to the test section is the ratio of the mass flow rate of vapor to the total mass flow rate. This is not the same as the ratio of vapor mass to total mass in the test section when the valves are shut.

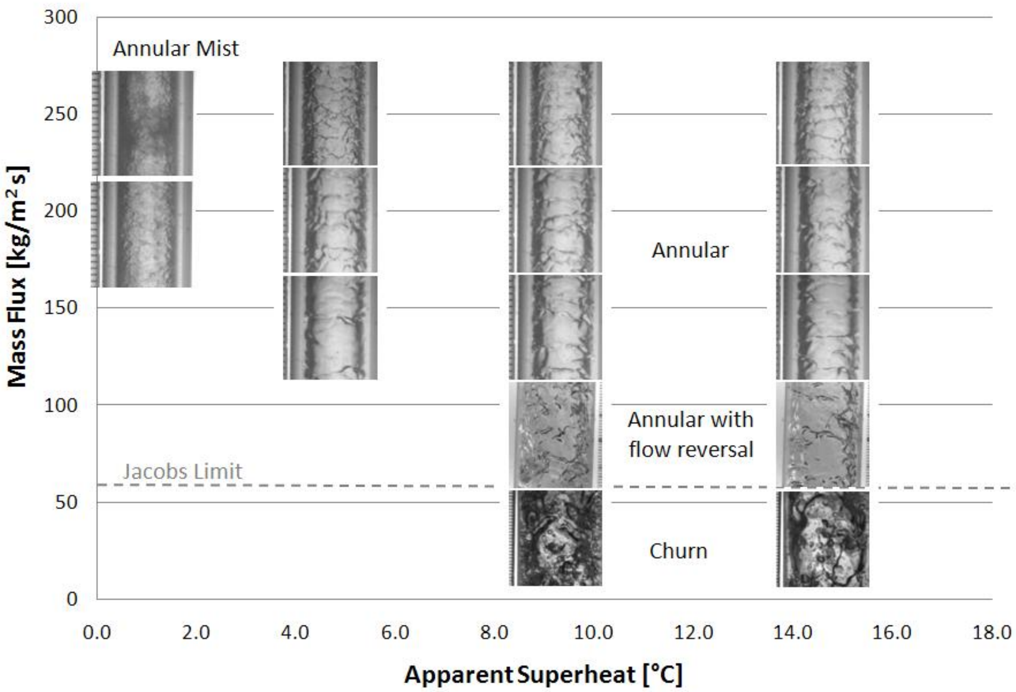

Figure 4-3 Visualization of vertical tube with 5% OCR

The effect of mass flux can once again be studied by comparing all the pictures in a single vertical column. The flow regime at high mass fluxes and high apparent superheat is annular with small ripples. This gives good oil return, because the entire liquid film is moving upwards and the oil film is thin. As the mass flux decreases, the film thickness and oil retention increase. The small ripples become larger waves in the pictures at 150 and 100 kg/m^2s, and some droplets are ripped off the tops of the waves and into the vapor core. At the Jacobs limit, the shear force from the vapor core reaches the limit of the liquid film it can support. Some of the liquid near the walls will actually flow downward, even thought the bulk flow is still upwards.

The Jacobs minimum recommend mass flux, which is described in the introduction, was calculated for the 18.5 mm tube with conditions at each apparent superheat value and is shown as a dotted line on Figures 4-3 and 4-4. When the mass flux decreases to below the Jacobs limit the “flooding” phenomenon occurs. The vapor shear is no longer able to support a liquid film and much of the liquid flows downwards and collects in the bottom of the vertical tube. A churn region appears at the bottom of the vertical tube, which is seen in the pictures for mass fluxes of 50 kg/m^{2}s in Figures 4-3 and 4-4. Above the churn region is a thin downward moving film on the walls and many droplets moving upwards in the core. The top of the churn region generates many droplets in the vapor core and these droplets are transported upwards along the tube. The turbulent flow causes some droplets to deposit onto the wall and form the downward moving liquid film, while the other droplets are transported up and out of the vertical section. The churn region looks similar for every OCR or mass flux; however the height of the region is dependent on these parameters. An increase in OCR or a decrease in mass flux will increase the height of the churn section.

The effect of the OCR can be seen by comparing Figures 4-3 and 4-4. Even at high mass fluxes, the OCR difference is more apparent in the vertical tube then in the horizontal tube. A noticeably thicker film is present at 5% OCR than at 1% OCR. The difference between the two OCRs remains consistent as mass flux decreases until the Jacobs limit. Once the flow transitions to the churn regime the effect of OCR becomes much more apparent in the vertical tube. The height of the churn region is dependent on OCR and mass flux, and an increase in OCR from 1% to 5%, or a decrease in the mass flux by 10 kg/m^{2}s will raise the height of churn region by about 0.5 m. The pressure drop is directly proportional to the height of the churn region, and the OCR effect below the Jacobs limit can be seen in Figure 4-13.

As the apparent superheat is reduced the amount of refrigerant in the liquid increases, changing the properties of the liquid and leading to the formation of some bubbles and droplets in the flow which can be seen in Figures 4-3 and 4-4. Once again, this annular mist flow regime is similar for either pipe orientation and for either OCR.

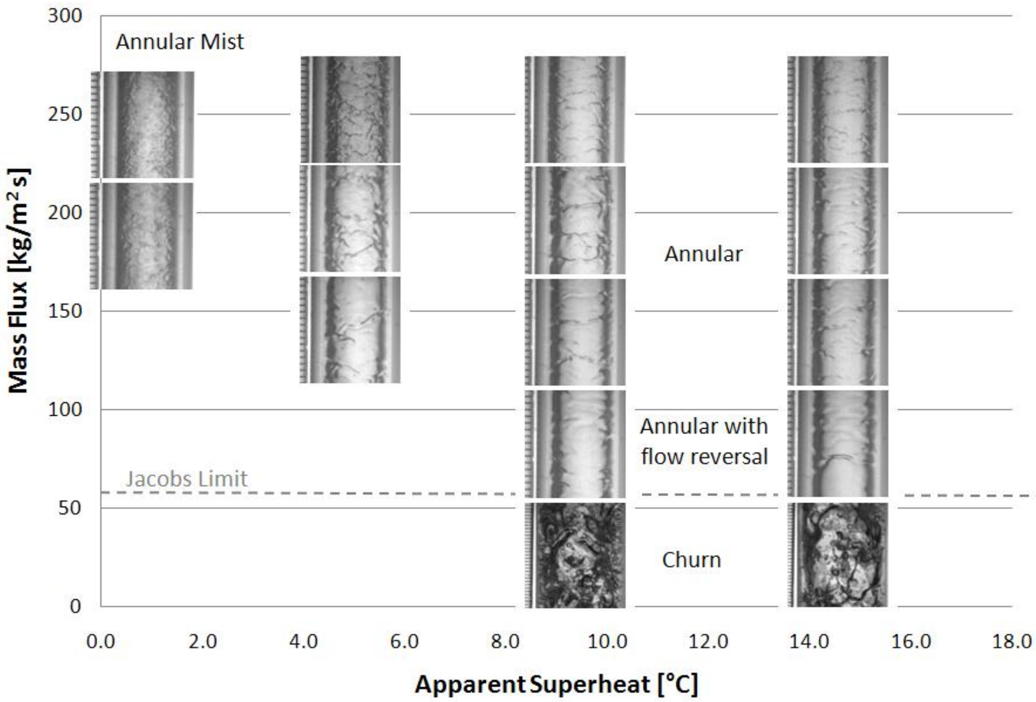

Figure 4-4 Visualization of vertical tube with 1% OCR

The Jacobs limit is empirically linked to the flooding phenomenon and the first formation of the churn flow regime at the bottom of the tube, as described in the introduction. The Jacobs limit is able to accurately predict the transition from annular to churn flow according to tests. However, there is some hysteresis in the flooding phenomenon which is important to note. Once the flow transitions to the churn regime the mass flux must be increased 20-30% above the Jacobs limit before it will transition back to annular flow. This transition region can be seen on Figure 4-5. The Jacobs limit does not account for this hysteresis, and therefore does not protect from high oil retention in churn flow in all cases. It is important to stay well above the Jacobs limit to avoid oil return problems due to hysteresis in the flow regime change.

4.4 Oil Retention

Figure 4-5 shows the relationship between oil retention per inner surface area and total mass flux. The data for this figure was taken at a saturation temperature of 12 °C with 15 °C of apparent superheat. The data for mass fluxes above 100 kg/m^{2}s were taken in the 7.2 mm pipe, and the data below 100 kg/m^{2}s were taken in the 18.5 mm pipe. The units for the ordinate were chosen to be grams of oil per internal surface area of the pipe. For annular flows, this method of plotting the mass of oil retained is effectively comparing the thickness of the film in each case, but does not completely account for the diameter effect, as may be seen in Figure 4-5. However, this method makes more sense than plotting oil retention per length [g/m] because the larger diameter pipe will retain much more oil per meter then the small pipe. Total mass flux of refrigerant and oil was chosen for the abscissa, in order to allow the addition of the Jacobs minimum mass flux. The mass flux is roughly proportional to vapor velocity throughout the range of OCR values tested.

Pictures of the flow regimes in the horizontal and vertical pipe are shown in the lower portion of the figure. These pictures correspond to the mass flux in each column, and were taken at 5% OCR and 15 °C apparent superheat. All pictures are of the 7.2 mm pipe, except for the two pictures at 50 kg/m^{2}s, which are of the 18.5 mm pipe.

The liquid forms a thin film on the walls of the pipe for conditions with high mass flux and high apparent superheat. The pictures on the right, the highest mass flux, are similar for the horizontal and vertical pipe. The similarity between the vertical and horizontal flow regimes is apparent in the graph; the oil retention for the vertical and horizontal flow is nearly identical at this high mass flux. OCR is shown through shade in the figure. An increase in the OCR from 3% to 5% results in increased oil retention of 20% to 50% for most cases.

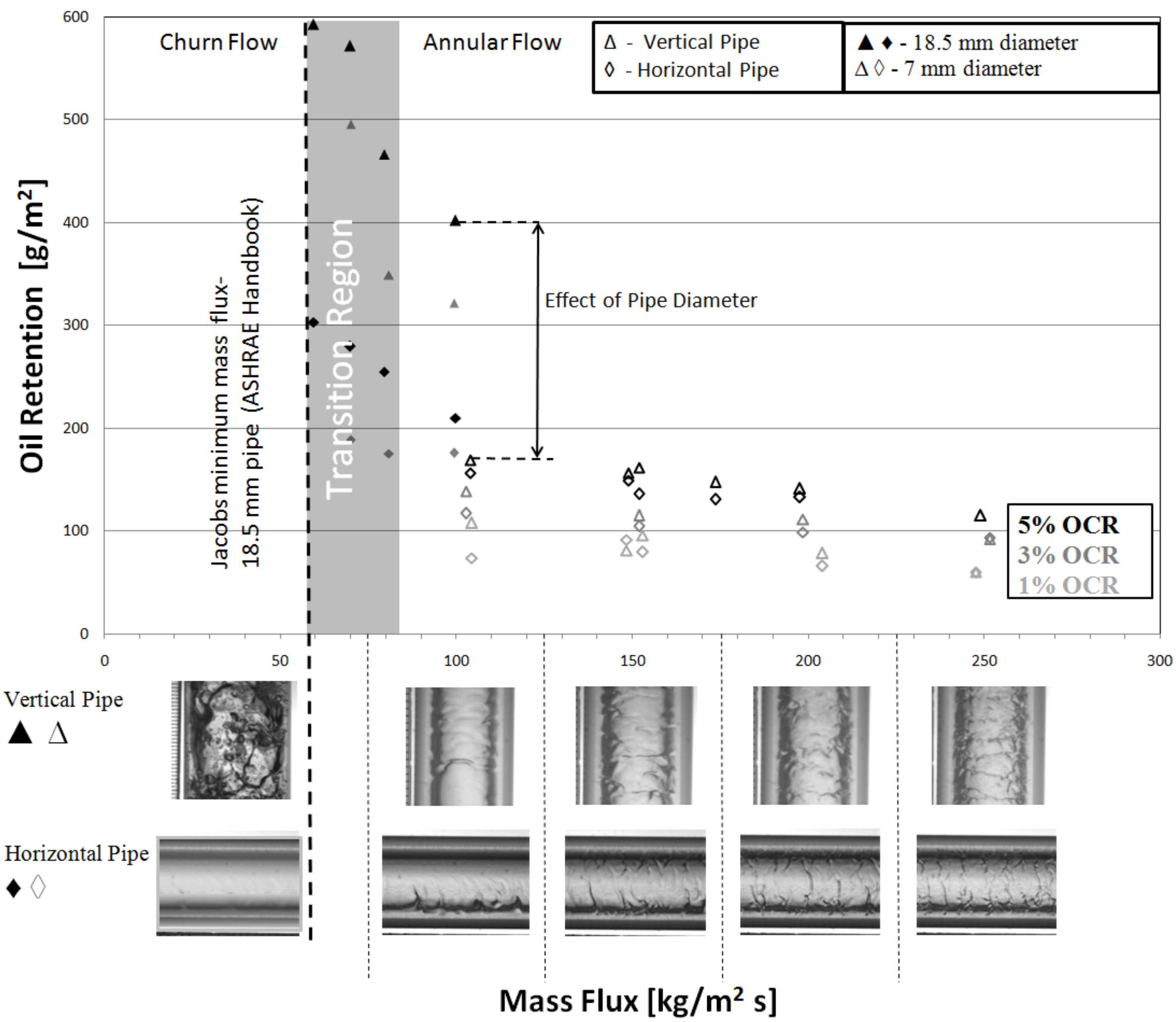

Figure 4-5 Oil Retention

The effect of pipe orientation becomes more apparent at mass fluxes below 150 kg/m^{2}s. The vertical pipe retains more oil as the shear force from the vapor core decreases. The gravity force on the liquid becomes more dominant, and a thicker film can be seen on the walls of the tube. The vertical tube retains more oil than the horizontal tube due to the different flow regimes. The horizontal pipe transitions to stratified flow at 100 kg/m^{2}s but the vertical pipe remains in annular flow with some recirculation of the liquid film. The oil retention in the vertical pipe has a steep negative slope at the Jacobs limit, while the horizontal pipe is more gradual. Gravity is working against the flow in the vertical pipe, unlike in the horizontal pipe.

Flooding occurs in the vertical pipe below 60 kg/m^2s, and the flow regime transitions to churn flow as can be seen in Figure 4-5, while the horizontal pipe remains stratified. The amount of oil retained in the vertical pipe will increase dramatically with any decrease in mass flux, or any increase in OCR. These same changes in the horizontal pipe will merely increase the thickness of the stratified liquid layer, and will not have as drastic effect on oil retention. The onset of flooding is predicted by the Jacobs flux; however there is some hysteresis in the flow regime transition. The mass flux must increase to approximately 80 kg/m^2s before the vertical pipe will return to annular flow. This transition region is not predicted by the Jacobs flux, and the increased oil retention due to the churn flow could be hazardous to the system.

Once the flow regime transitions to churn, much of the liquid falls to the bottom of the vertical tube, and forms a column. As described earlier, the height of this churn column is dependent on OCR and mass flux. It is difficult to generalize the oil retention in churn flow, because the churn column and the falling annular section above have different oil retention rates. Thus the oil retention in each section must be characterized, as well as the height of the churn column. No oil retention data was taken in the churn flow regime, as can be seen on Figure 4-5, but a method of characterizing this oil retention is currently in the works.

It can be seen in Figure 4-5 that there is a large diameter influence on the oil retention per surface area in the vertical tube. As mentioned previously, oil retention per surface area is the average film thickness in annular flows. The effect of diameter on dimensionless film thickness, shown by expression 4.1, can be correlated to the liquid film Reynolds number, given by equation 4.2, using equation 4.3 (Van Rossum, 1959). These dimensionless parameters were derived from a force balance on a thin laminar liquid film in ideal flow conditions, as explained by Van Rossum (1959).

$$\frac{\delta_o}{\nu_l}\left(\frac{\tau_i}{\rho_l}\right)^{0.5} = Dimensionless\ film\ thickness\ parameter \tag{4.1}$$

$$Re_l = 4q/\nu_l \tag{4.2}$$

In these equations, τ_i is the interfacial shear stress between the liquid film and vapor core, ν_l is the liquid kinematic viscosity, ρ_l is liquid density, and *q* is the volumetric flow rate of liquid divided by the circumference of the tube. Van Rossum (1959) used a correction factor of $\delta/0.6 = \delta_o$ because the shear stress of the liquid film at the wall was used, instead of at the liquid-vapor interface. In the current study, the shear stress was calculated using equation 4.3, with the interfacial friction factor coming from equation 4.4 (Wallis, 1969). Although the shear stress was calculated between the liquid and vapor, a correction factor of $\delta/1.2 = \delta_o$ was used to account for the smooth circular channel. This correction factor may need to be adjusted for other geometries, such as internally grooved pipes.

$$\tau_i = 0.5(f_i)(\rho_v)(u_v)^2 \tag{4.3}$$

$$f_i = .005(1 + 300\left(\frac{\delta}{D}\right)) \tag{4.4}$$

The dimensionless liquid film thickness parameter and liquid Reynolds number were calculated for all experimental data, and for horizontal and vertical tubes are plotted in Figures 4-

6 and 4-7, respectively. These data are accompanied by results taken from Cremaschi (2004) for R410A/POE in the vertical suction line, as well as R410A/POE and R410A/MO in the horizontal suction line. The data shown came from a range of experiments consisting of diameters from 7.2 to 19 mm, mass fluxes from 80 to 250 kg/m^{2}s, apparent superheats from 5 to 20 °C, and liquid viscosities from 2 to 28 cSt.

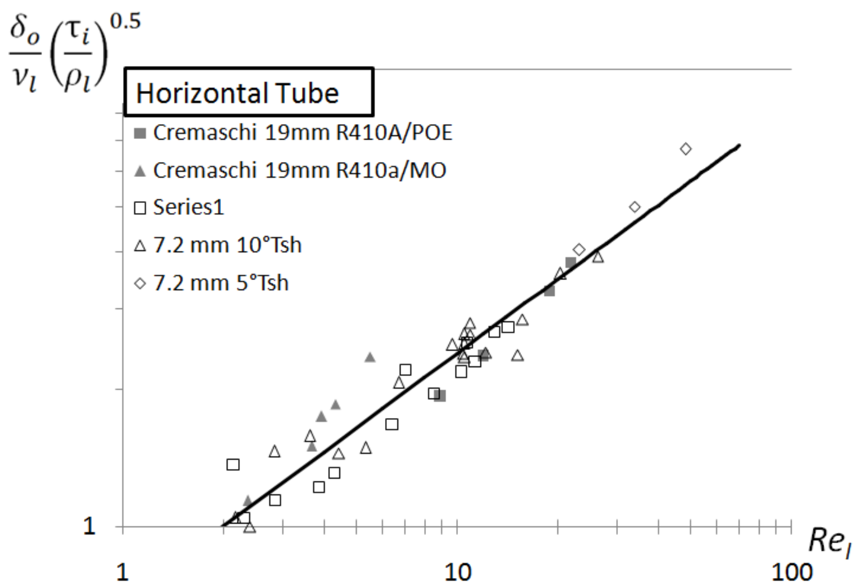

Figure 4-6 Film thickness diameter correction, horizontal tube

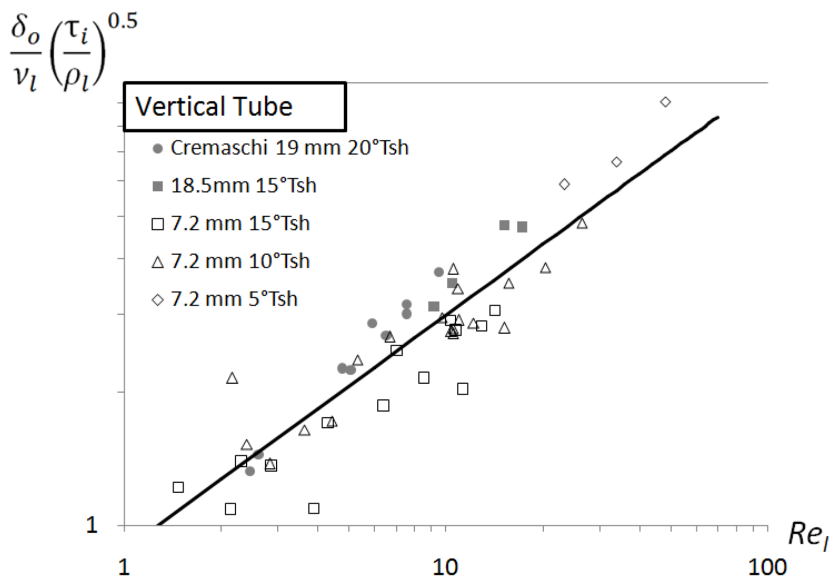

Figure 4-7 Film thickness diameter correction, vertical tube

The data in Figures 4-6 and 4-7 was a least squared curve fit was applied to the non-dimensional terms proposed by Van Rossum (1959), and the curve equations can be used to calculate film thickness if all other parameters are known. The equations which relate the film thickness parameter to the liquid film Reynolds number are shown below.

$$\frac{\delta_o}{\nu_l}\left(\frac{\tau_i}{\rho_l}\right)^{0.5} = 0.69\ Re_l^{0.54} \quad \text{(Horizontal Tube)} \tag{4.5}$$

$$\frac{\delta_o}{\nu_l}\left(\frac{\tau_i}{\rho_l}\right)^{0.5} = 0.88\ Re_l^{0.53} \quad \text{(Vertical Tube)} \tag{4.6}$$

The correlation works well for the immiscible combination of R410A/MO, where the liquid viscosity was taken to be 28 cSt. The flow regime must be annular for the film thickness parameter to be calculated.

Solving these equations for the corrected film thickness, δ_o, gives relationships which can be used to predict the annular film thickness in the suction line, equations 4.7 and 4.8. These should only be applied when the flow is in the annular regime. Equation 4.9 can be used to calculate the amount of oil retention in a system from the calculated film thickness.

$$\delta_o = 0.69 \nu_l \, Re_l^{0.54} * \left(\frac{\rho_l}{\tau_i}\right)^{0.5} \quad \text{(Horizontal Tube)} \tag{4.7}$$

$$\delta_o = 0.88 \nu_l \, Re_l^{0.53} * \left(\frac{\rho_l}{\tau_i}\right)^{0.5} \quad \text{(Vertical Tube)} \tag{4.8}$$

$$m_{oil\,retention} = \delta * \pi D * L * \rho_l * w_{local} \tag{4.9}$$

The interfacial shear stress is dependent on the film thickness, as shown in equation 4.4. Therefore a guess value must be used for either δ_o or τ_i, and an answer may be calculated using an iterative method. Once δ_o is obtained, δ can be calculated using the correction factor of 1.2 and the mass of oil in the suction line can be estimated from using equation 4.9. Equations 4.7 and 4.8 were able to predict the experimental data from the current experiment, as well as from Cremaschi (2004), with an average error of 10.9% for the vertical tube, and 7.9% for the horizontal tube. Figures 4-8 and 4-9 show a comparison of calculated oil retention to actual measured oil retention in both the vertical and horizontal suction lines.

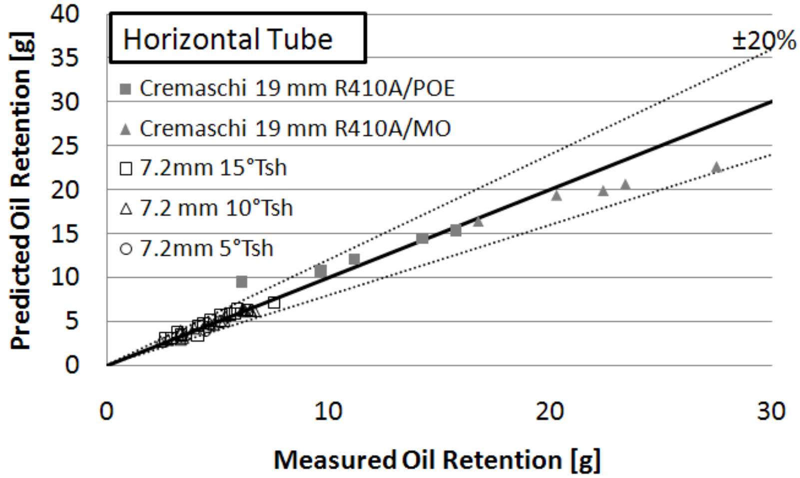

Figure 4-8 Predicted vs experimental oil retention in the horizontal suction line

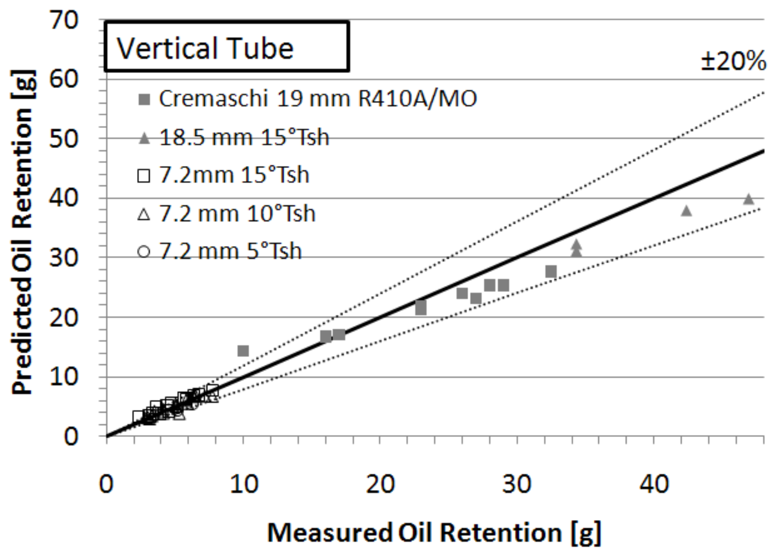

Figure 4-9 Predicted vs experimental oil retention in the vertical suction line

Figure 4-10 shows the performance of the three most recent oil retention prediction methods, Radermacher (2006), Crompton (2004), and the method proposed in this paper. The prediction lines are drawn for 3% OCR in the 7.2 mm horizontal tube, as well as 3% and 5% OCR in the 18.5 mm vertical tube. The Radermacher (2006) and Crompton (2004) methods both are only able to predict oil retention in the horizontal suction line. They both under-predict the mass of oil retained by nearly 50%, as can be seen in the figure. The new oil prediction method is able to predict oil retention for both pipe diameters as well as the vertical and horizontal suction lines to within 10%. No predictions are made for the horizontal 18.5 mm tube, since the flow is stratified for all data points taken, and the predictions are only valid for annular flow. The predictions do not stretch into the transition region, due to the possibility of churn flow, and the increased oil retention from recirculation of the liquid film.

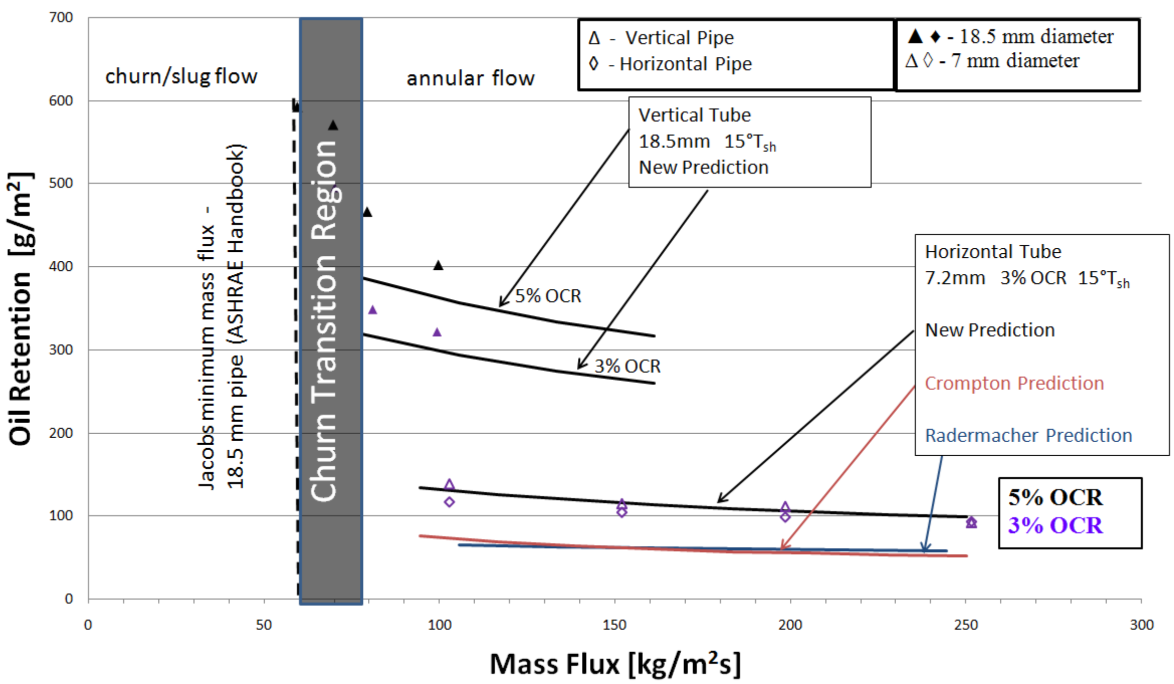

Figure 4-10 A comparison of three oil retention prediction methods

4.5 Effects of Apparent Superheat

The effect of changing the apparent superheat is shown in Table 4-2 and Figures 4-11 and 4-12. There are two conflicting effects which influence the viscosity of the liquid phase. More refrigerant evaporates out of the liquid as apparent superheat is increased. This causes the liquid to become more oil-rich, and thus increases the viscosity. The mass fraction of oil in the liquid is shown in the 2nd column of table 4-2 and the concentration of oil increases from 60% to 77%

with an apparent superheat increase from 5 °C to 15 °C. The conflicting effect is the viscosity of the oil as a function of temperature. The 4th column shows that the viscosity of pure oil decreases significantly as the temperature is increased. The dominant factor is the change in oil concentration in the liquid, which leads to an overall increase in viscosity as apparent superheat increases as shown in the 5th column.

Table 4-2 Relationship between viscosity and apparent superheat[1]

Apparent Superheat[1]	Concentration of Oil in Liquid[2]	Viscosity of Pure Refrigerant Liquid[3]	Viscosity of Pure Oil[4]	Viscosity of Liquid Mixture[4]
[°C]		[cP]	[cP]	[cP] = 0.001 [Pa·s]
5	0.5983	0.13	73	2.2
10	0.7051	0.13	58	5.1
15	0.7684	0.12	46	6.9

[1] Values calculated for a saturation temperature of 12°C
[2] Calculated using the Takaishi & Oguchi (1987) T_{bub} method shown in section 3
[3] Calculated using Engineering Equation Solver
[4] Data from Cavestri & Schafer (2000), R410A / POE 32 ISO

Changing the apparent superheat at the inlet to the test section influences oil retention through the change in viscosity. Higher viscosity liquids form a thicker film on the tube walls, thus increasing oil retention. Increasing the apparent superheat from 5 °C to 15 °C increases the viscosity by 4.7 cP. The effect on oil retention is small but noticeable as Figures 4-11 and 4-12 illustrate. Figure 4-11 shows an increase in oil retention by 18 g/m^2, or 15%, with an apparent superheat increase from 5 °C to 15 °C. This decrease is not as noticeable in Figure 4-12, because it is on the same order as the variability of the mass measurements.

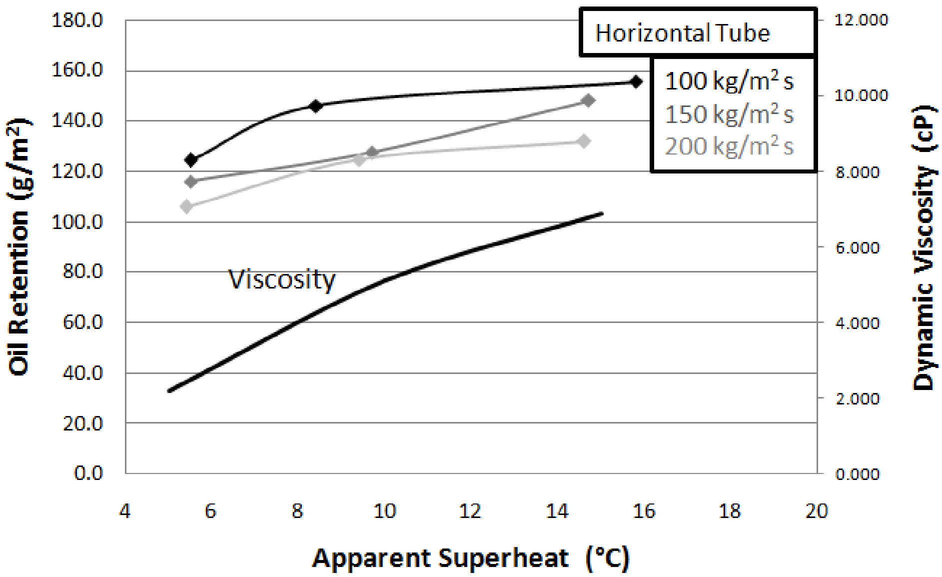

Figure 4-11 The effect of apparent superheat on oil retention in the horizontal tube

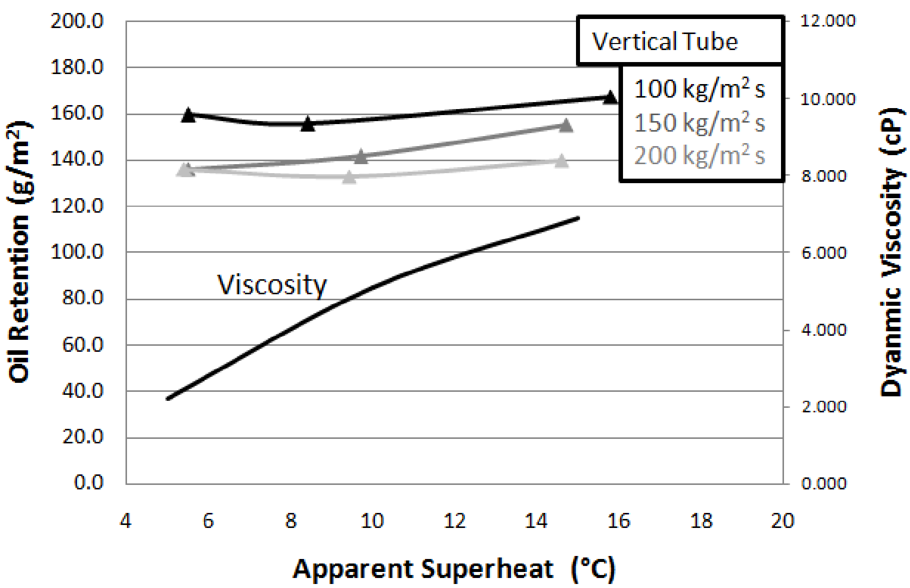

Figure 4-12 The effect of apparent superheat on oil retention in the vertical tube

4.6 Pressure Drop

Figure 4-13 shows the pressure drop per unit length in the vertical and horizontal suction lines. The data for this figure was also taken at a saturation pressure corresponding to a temperature of 12 °C with 15 °C of apparent superheat. Pressure drop measurements taken for pure refrigerant at a quality of 0.95 in the 7.2 mm tube are also shown on the figure, along with the Friedel two phase pressure drop prediction. These tests verified the accuracy of the pressure drop measurements.

In the high max flux conditions shown in the diagram, which is the annular regime, interfacial friction dominates the pressure drop. In this region, increases in flow rate will increase the Reynolds number, and thus increase the overall pressure drop.

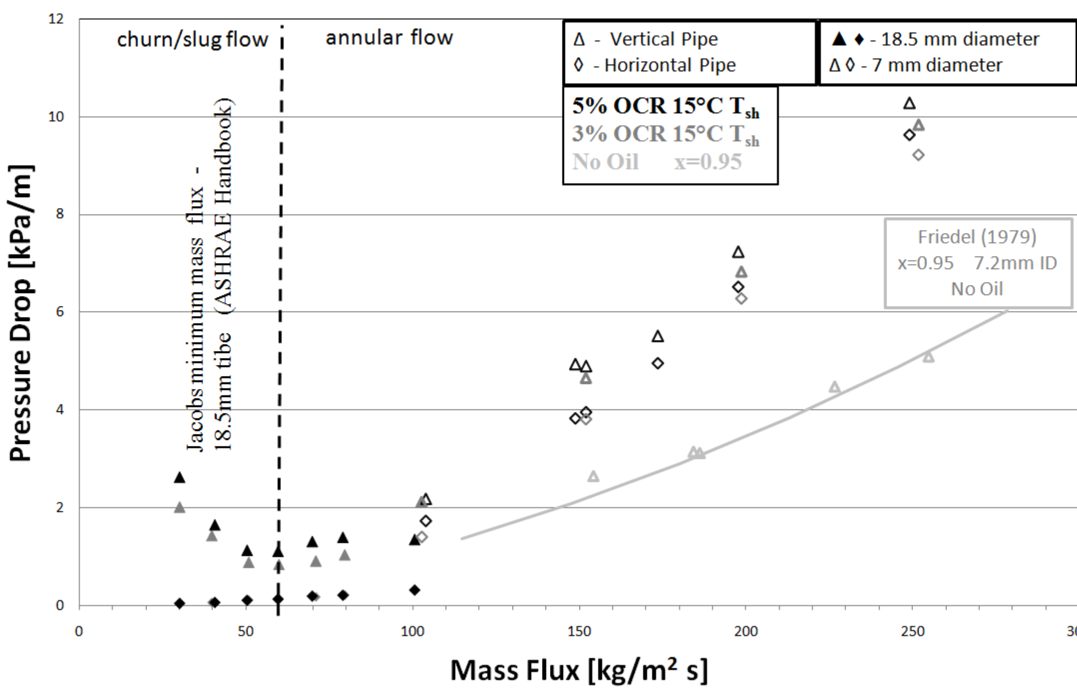

Figure 4-13 Pressure Drop

The pressure drop in the horizontal and vertical tubes is nearly identical for all mass fluxes above the Jacobs limit, because the flow regimes are very similar. The gravitational force on the liquid in the vertical tube causes the pressure drop to always be slightly higher than the horizontal tube. As the flow rates approach the Jacobs limit, the pressure drop in the vertical tube reaches a minimum at the transition to the churn regime. Below this mass flux, pressure drop becomes dominated by the hydrostatic force of the liquid column. The churn region increases in height with decreasing mass flux, therefore the hydrostatic force, and consequently the pressure drop, will also increase.

Immediately after the mass flux drops below the Jacobs limit and the flow regimes change to churn flow, the churn region is very short, and changes in OCR will not have much effect on the height of the region. This is why the effect of OCR is not very apparent at mass fluxes around the Jacobs limit. However, as mass flux decreases and the churn region increases in height, changes in OCR have a greater effect on the churn region height, and thus on the pressure drop in the vertical tube.

The horizontal tube maintains stratified flow for all low mass fluxes, thus pressure drop continues to decrease with decreasing mass flux. Increases in OCR have minimal effect on pressure drop in the horizontal tube, because they have such a small effect on the liquid layer.

4.7 Repeatability:

The mass measurement of a single test condition was repeated 5 times over the course of two weeks in order to test the repeatability of the measurement procedure and experimental setup. The important conditions and mass measurements of the tests are shown in Table 4-3.

Table 4-3 Repeatability Test 7.1mm Tube

Saturation Temperature	Mass Flux	OCR	Temperature Vapor Core	Temperature Tube Wall	Mass of Oil Horizontal Tube	Mass of Oil Vertical Tube
[°C]	[kg / m^2 s]		[°C]	[°C]	[g / m]	[g / m]
12.1	101.8	0.048	22.10	21.60	6.22	6.16
12.2	101.2	0.050	22.10	21.80	6.35	6.54
12.1	101.3	0.049	22.10	21.80	6.35	6.08
12.4	100.7	0.050	21.80	21.50	6.89	7.37
12.2	102.5	0.051	22.10	21.70	6.54	6.61

The saturation temperature was calculated from the saturation pressure measured at the inlet of the test section. The total mass flux of refrigerant and oil is shown, along with the OCR. The temperature at the exit of the evaporator was measured in two locations as described before, in the center of the tube, T_core, and on the outside of the tube wall, T_wall. The two temperatures are close together, indicating that the liquid and vapor phases are near equilibrium. The small difference in temperature has a minor effect on liquid properties equilibrium conditions are assumed. The apparent superheat is the difference between the saturation temperature and the measured wall temperature, and is approximately 10 °C for all cases.

The average oil retention for the horizontal tube is 6.47 g/m and for the vertical tube is 6.55 g/m. The standard deviation of each test is a good measure of the repeatability, 0.26 g/m for the horizontal tube, and 0.51 g/m for the vertical tube. The standard deviation of the vertical tube is 7.8% of the average mass measurement for that tube. This variability stems from many sources. The error in the instruments contributed to the overall variation of each data point. If the valves were not closed at nearly the same time, some excess oil may have entered or left the test section, which could have generated errors in the measurements. The slight differences in mass flux, OCR, and saturation temperature could cause variation in the mass retention. Finally the flow of the liquid film is unsteady at any condition, which would cause variation in mass measurements even if all the inlet conditions were held perfectly steady. This unsteadiness can be seen by watching the liquid film in the pipes, or through high speed recordings of the flow. All of these factors combined affect the repeatability of each test condition.

5 CONCLUSIONS

- Oil retention increases substantially in the vertical tube when the liquid film begins to flow downwards. This mass flux where recirculation begins is above the Jacobs limit. As long as the compressor contains enough oil to make up for the retention in the suction line these flow regimes are acceptable.
- The Jacobs limit predicts the onset of flooding and the churn flow regime. However, there is some hysteresis in the regime change and the regime will not transition back to annular until mass fluxes 30% above the Jacobs limit. In special cases, this could become problematic for oil return in systems, and should be noted.
- The Jacobs limit should be used in conjunction with the oil retention correlations provided for sizing suction risers and charging oil in the compressor. The correlations were able to predict oil retention with 10.9% average error in the vertical tube and 7.9% average error in the horizontal tube.
- The OCR has a significant effect on the oil retention in the suction line. Increasing the OCR from 1% to 3% leads to a 20% to 50% increase in oil retention in all cases. An oil separator at the exit of the compressor may be a feasible method to reduce overall OCR if oil retention is problematic in a system.
- The vertical suction line tends to retain 10% more oil than the horizontal line when both pipes are in the annular flow regime. However, once the horizontal line transitions to stratified flow the difference becomes more apparent. Near the

Jacobs limit, the vertical suction line retains twice as much oil as the horizontal line.

- A 5 °C increase in apparent superheat causes a 15% increase in oil retention in the apparent superheat range studied. At higher apparent superheats more refrigerant is evaporated from the liquid, which increases the mass fraction of oil in the liquid, and thus the viscosity. Higher viscosity liquids will form a thicker film on the tube wall, and retain more oil.

REFERENCES

Burr, J., Newell, T., & Hrnjak, P. (2005). Experimental Investigation of Viscous Two-Phase Flow in Microchannels. *ACRC Technical Report 252* .

Cavestri, R., & Schafer, W. (2000). Measurement of Solubility, Viscosity, and Density of R410A Refrigerant/Lubricant Mixtures. *ASHRAE Transactions Vol 106* , 277-285.

Cremaschi, L. (2004). Experimental and theoretical investigation of oil retention in vapor compression systems. *PhD Thesis, University of Maryland* .

Cremaschi, L., Hwang, Y., & Radermacher, R. (2005). Experimental Investigation of Oil Retention in Air Conditioning Systems. *International Journal of Refrigeration 28* , 1018-1028.

Crompton, J., Newell, T., & Chato, J. (2004). Experimental Measurement and Modeling of Oil Holdup. *Masters Thesis, University of Illinois* .

Hajal, J., Thome, J., & Cavallini, A. (2003). Condensation in horizontal tubes, part 1: two-phase flow pattern map. *International Journal of Heat and Mass Transfer #46* , 3349-3363.

Jacobs, M., Scheideman, F., Kazem, S., & Macken, N. (1976). Oil Transport by Refrigerant Vapor. *ASHRAE Transactions* , 318-329.

Jassim, E., & Newell, T. (2005). Prediction of Two-Phase Pressure Drop and Void Fraction in Microchannels Using Probabilistic Flow Regime Mapping. *ACRC Technical Report 241* .

Lee, J.-P., Hwang, Y., Radermacher, R., & Mehendale, S. (2001). Experimental investigations on oil accumulation characteristics in a vertical suction line. *ASME Int. Mechanical Engineering Congress and Expo. AES-Vol 41* , 63-69.

Mehendale, S. (1998). Experimental and Theoretical Investigation of Annular Film Flow Reversal in a Vertical Pipe. *PhD Dissertation, University of Maryland* .

Mehendale, S., & Radermacher, R. (2000). Experimental and Theoretical Investigation of Annular Film Flow Reversal In a Vertical Pipe: Application To Oil Return In Refrigeration Systems. *HVAC&R Research, Vol. 6, No. 1* , 55-74.

Radermacher, R., Cremaschi, L., & Schwentker, R. A. (2006). Modeling of Oil Retention in the Suction Line and Evaporator of Air-Conditioning Systems. *HVAC&R Research, Vol 12, No. 1* , 35-56.

Ray, S. (1988). *Applied Photographic Optics.* London: Focal Press.

Sheth, V., & Newell, T. (2005). Refrigerant and Oil Migration and Retention in Air Conditioning and Refrigeration Systems. *ACRC Technical Report 240* .

Takaishi, Y., & Oguchi, K. (n.d.). Measurements of vapor pressures of R22/oil solution. *Proceedings of the 18th International Congress of Refrigeration* , 217-222.

Thome, J. R. (1995). Comprehensive Thermodynamic Approach to Modeling Refrigerant-Lubricating Oil Mixtures. *HVAC&R Research, Vol. 1, No. 2* , 110-125.

Van Rossum, J. J. (1959). Experimental Investigation of Horizontal Liquid Films. *Chemical Engineering Science Vol 2* , 35-52.

Wallis, G. (1969). *One Dimensional Two-Phase Flow.* New York, NY: McGraw-Hill Book Company.

APPENDIX A

Detailed Component List

Table A-1 Instrumentation

Measurement	Device Description	Range	Error +/-
Absolute Pressure Transducer	Honeywell TJE 2049-16-01	0-500 psia	1.25 psi
		(0-3447 kPa)	(8.6 kPa)
Horizontal Differential Pressure Transducer	Honeywell Mod. Z -5556-03	0 +/- 10 psi	0.025 psi
		(0 +/-68.98 kpa)	0.1 kPa
Vertical Differential Pressure Transducer	Honeywell Mod. Z-5556-05	0 +/- 15 psi	0.0375 psi
		(0 +/-103.4 kPa)	(0.26 kPa)
Refrigerant Mass Flow Rate	MicroMotion CMF 25 Coriolis Effect Mass Flow Meter	Max 605 g/s	0.15% of rate
		Calibration 0-30 g/s	typ: 0.02 g/s
Refrigerant Density		na	0.5 kg/m^3
Oil Mass Flow Rate	MicroMotion CMF10 Coriolis Effect Mass Flow Meter	Max 30 g/s	0.15% of rate
		Calibration 0-10 g/s	typ: 0.002 g/s
Oil Density		na	0.5 kg/m^3
Water Mass Flow Rate	MicroMotion CMF 25 Coriolis Effect Mass Flow Meter	605 g/s	0.15% of rate
			typ: 0.2 g/s
Balance	AND Electronic Balance FP-6000	6100 g	0.03 g
			(stdev of test)
Temperature	Omega Type-T Welded Thermocouple	-250 to 400 °C	0.5°C

Table A-2 Components

Component	Description	Specifications
Helical Liquid Separator	Henry Tech S-5185	Internal volume 3.1 L
		Nominal Volume Flux 4 CFM
Refrigerant Condenser	AIA 26 Plate Heat Exchanger	0.071 m^2 per plate
Refrigerant Subcooler	Generic 10 Plate Heat Exchanger	0.03 m^2 per plate
Refrigerant Pump	MicroPump S-1385 Gear Pump	Toshiba VFSX 2007P Variable Frequency Inverter, 230VAC, 1-240 Hz
	Driven by Magnatec 3ph, 1hp AC motor	
Oil Subcooler	Generic 10 Plate Heat Exchanger	0.03 m^2 per plate
Oil Pump	Micropump 82003	Fixed Frequency Motor with Bypass Valve
	Driven by Magnatec 1 ph, 0.25 hp AC motor	
Evaporator	AIA 26 Plate Heat Exchanger	0.071 m^2 per plate

Data Acquisition System

All of the instruments used in the experimental setup were monitored with a data acquisition system. A Yokogawa HR1300 hybrid data logger was used to measure the output signals of the thermocouples, pressure transducers, and mass flow meters. It uses a Yokogawa original high breakdown voltage solid state relay, which scans at a rate of 10 points per second. The strip recorder was not used, since the data logger interfaces directly with a computer.

Figure A-1 Yokogawa HR 1300 Hybrid Data Logger

The resolution of the Yokogawa data loggers voltage measurement is lower than the associated error in all cases, and therefore the only the instrument error is presented in Tables A-1 and A-2.

The mass flow meters output a current signal between 4 and 20mA, for a programmable range of mass flux and density. The programmed ranges are shown in the table above. The current signal was read by the data logger as a voltage across a 250Ω resistor, resulting in a voltage reading between 1 and 5 V. The accuracy of the voltage measurement by the data logger in this range was 0.05% of the reading, with a resolution of 1mV. The three pressure transducers output a direct voltage signal between 0 and 20 mV over their respective pressure range. The accuracy of the voltage measurement by the data logger for this voltage range is 0.05% of the reading, with a resolution of 1 μV. All three pressure transducers were calibrated using no less than 15 points and their respective outputs on the data logger. The calibration equation is applied in the LabVIEW program. The thermocouples were directly read by the data logger with an accuracy of 0.5 °C.

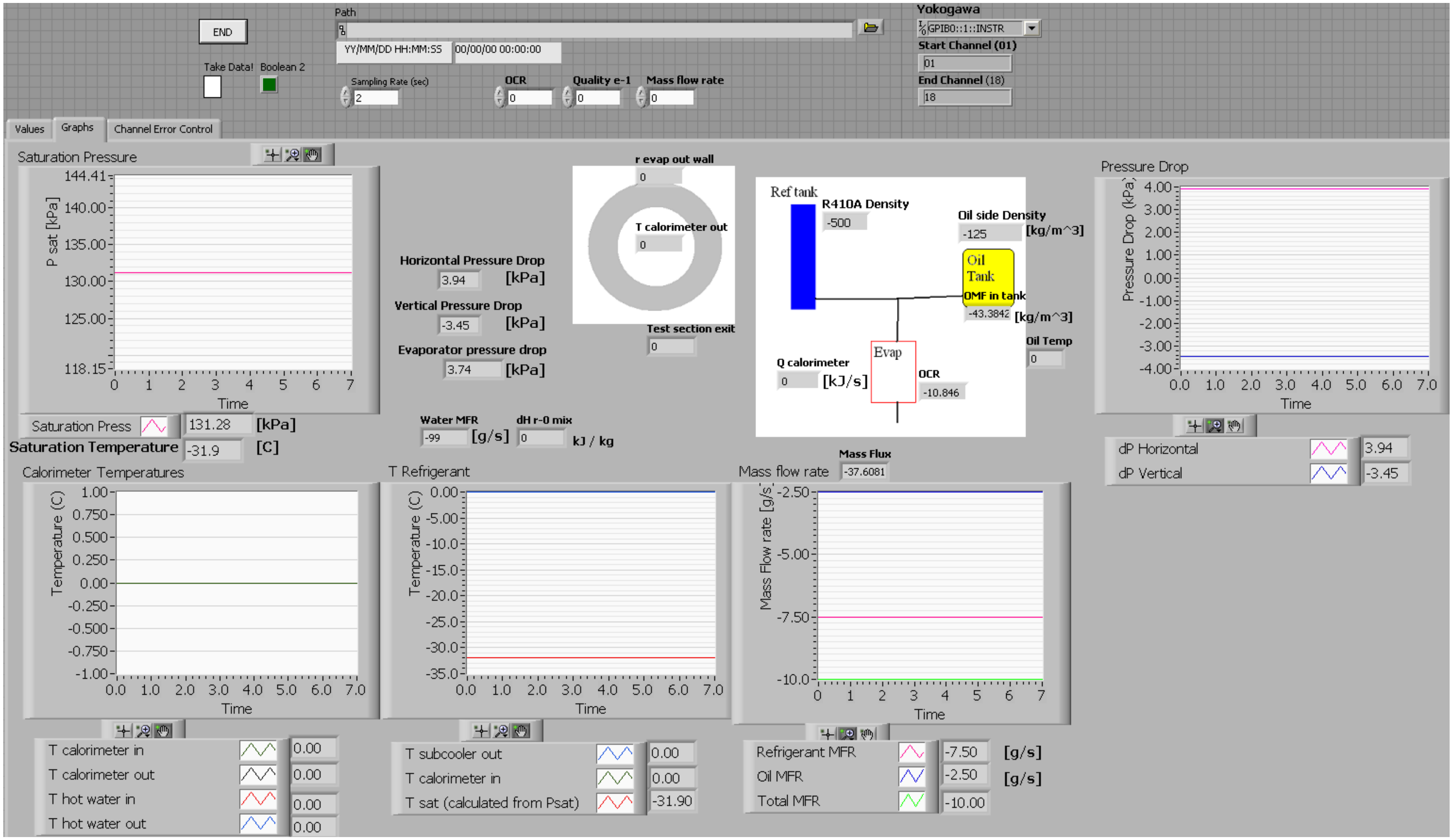

Figure A-2 LabVIEW Interface

The Yokogawa data logger was connected to a PC via a serial interface. A National Instruments GPIB IEEE 488.2 PCI card read the signal from the data logger, and communicated directly with the LabVIEW program. The front panel of the LabVIEW program used is shown in Figure B-1. When activated, data was taken at two second intervals and recorded in an excel spreadsheet for analysis.

Test Section

The experimental setup had two separate test sections, one to simulate the horizontal suction line, and one to simulate the vertical suction line. The test sections were made out of clear PVC pipe to allow visualization of the entire flow regime inside of the pipe. The inner diameter of the tube was constant from the inlet of the 50 diameter development length to the inlet of the liquid separator. The segment above the vertical test section had a constant diameter all the way through the vertical u-bend and into a downward flowing section before the separator. This was to eliminate any flow disturbances which may have affected the pressure drop or oil retention measurements.

Test sections with two different diameters were built so a wide range of mass fluxes could be tested. The specifications of the PVC pipe used for the test sections are shown in Table A-3.

Table A-3 Test Section Specifications

Inner Diameter (mm)	Nominal Size (in)	Schedule	Outer Diameter (mm)	Max Pressure (kPa)
7.1	1/4	80	13.7	3930
18.5	3/4	80	26.7	2344

The test sections consisted of the clear PVC pipe section with a special coupling to convert from the PVC to a metal NPT connection and a valve on either side. Ball valves were used for two reasons, they could be quickly closed for trapping the refrigerant and oil during experiments, and they provided a nearly constant inner diameter when completely open. Care was taken to minimize any gaps along the inner diameter of the test section. This eliminated any pressure drop or excess oil retention resulting from flow disturbances. Minor losses were calculated for any small gaps that may have occurred, and their pressure drop was an order of magnitude lower than the frictional pressured drop across the test section.

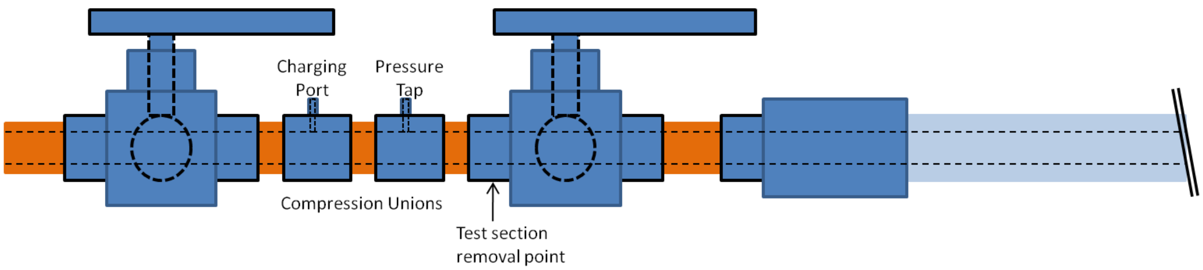

Figure A-3 Entrance to the horizontal test section

The entrance to the horizontal test section is shown above. The two valves in this section were sized appropriately, such that the inner diameter was nearly the same as the copper and PVC tubes. The valves used compression fittings, as shown in Figure A-4 which allowed easy removal and replacement of the test section for mass measurements. The valves were closed simultaneously when a mass measurement is taken. The valve shown on the left seals the system off from the atmosphere, and the valve on the right seals the test section off from the atmosphere. The charging port and pressure tap were both made from union compression fittings as shown in Figure A-5. A small hole, 1/32 inch with a 1/8 inch countersink, was drilled through the fitting, and then a piece of 1/8 inch copper pipe was brazed over the hole. This allows pressure measurements with virtually no flow disturbance. The pressure between the two valves was released through the charging port, and then the test section could be removed for weighing.

After the test section was reinstalled, the air was vacuumed through the charging port, and then the test section was pressurized with refrigerant. This way no air entered the system.

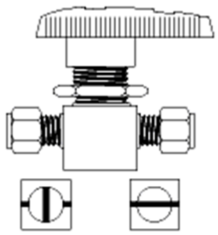

Figure A-4 Ball Valve

Figure A-5 Union Fitting

The test sections were removed from the experimental apparatus, and were then prepared for weighing. They were wiped down to remove any dirt or oil from the outside. The open end of the valve was cleaned out, and the valve was wiped off as well. The PVC pipe test section was not able to support the heavy valves at either end when sitting on a scale. Lightweight foam sheathes were constructed to hold the test sections on the scale and avoid placing excess stress on the tubes. Two sheathes were made for the small diameter test section, since the ¼ inch PVC was not very stable. The ¾ inch test section was placed on top of one of the sheaths for extra support during weighing. The mass of each sheath alone was taken before every measurement, to ensure accuracy. A table with the dimensions of the test sections, as well as the typical sheath weights is shown below.

Table A-4 Test Section Dimensions

Inner Diameter (mm)	Orientation	Length (m)	Tare Weight (g)	Sheath Weight (g)
7.1	Horizontal	2.02	1305	509.18
	Vertical	1.92	1210	479.41
18.5	Horizontal	1.63	2943	509.18
	Vertical	1.81	3004	509.18

Flow Visualizations

The test sections were built with clear PVC pipe so the flow regimes in the horizontal and vertical test sections could be studied. A method of capturing sharp images of the tubes was necessary for documenting the flow conditions. A standard digital camcorder or webcam was one potential for documenting the flow regimes. These types of cameras have typical frame rates of 30 to 60 frames per second. In most of the flow conditions studied, the vapor velocity is between 2 and 3 m/s. At these frame rates, a droplet moving at the vapor velocity could potentially travel 50mm between frames. It would be impossible to capture smooth movements of the flow structures at these frame rates. In addition, the shutter speed of standard cameras is not always adjustable and the images may appear blurry if the exposure time is too long. For these reasons, a high speed camera was chosen for the visualization of the flow regimes.

Figure A-6 Vision Research Phantom v4.2 high speed camera

The high speed camera used was a Vision Research, Phantom v4.2 shown in Figure A-6. It is capable of taking images at a maximum of 2100 frames per second with the full resolution of 512 x 512 pixels. The camera can take images at higher frame rates with lower resolution, because less information is stored for each frame. Experimental videos were shot with a resolution of 256 x 256, and a frame speed of 3000 fps, in order to capture the flow details. Table A-5 shows some examples of maximum frame rates for various resolution settings.

The monochromatic SR-CMOS sensor can store each pixel with an 8 bit depth, meaning there are 2^8 or 256 different shades of gray that the camera can record. Completely black pixels receive a value of 0, and shades between black and saturated white are converted linearly from 1 to 255. The exposure time of each frame can be varied from 2 µs to just less than the inverse of the frame rate. A shorter exposure time will let in less light, causing the average pixel brightness to drop. However, a shorter exposure time will also produce a sharper image, especially for fast moving objects. For example, an object moving at 3 m/s will move 1.5 mm during an exposure time of 500 µs. The object will appear elongated by 1.5 mm in that frame, which could lead to some confusion about the actual shape of the object. If the exposure time is shortened to 30 µs, the object will move only 0.09 mm in the frame, thus appearing very sharp. However, this faster exposure time requires 17 times the amount of light to resolve the image. It was therefore necessary to use large, bright lights when recording fast moving flow regimes.

Table A-5 Maximum Frame Rates

Resolution (Pixels)	Max. Frame Rate (fps)
512 x 512	2,100
512 x 384	2,840
512 x 256	4,219
512 x 128	8,196
512 x 64	15,625
320 x 240	6,622
256 x 512	4,219
256 x 256	7,407
256 x 128	9,708
256 x 64	14,285
160 x 120	25,641
128 x 128	20,408
128 x 64	38,461
64 x 64	52,631
32 x 32	90,000

The high speed camera is operated using proprietary software distributed by Vision Research called Phantom Camera Control. A screenshot of the software is shown in Figure A-7. The software allows for the adjustment of the frame rate, exposure time, and resolution, and is used to adjust the triggering process. Once the parameters are set, the video capture mode is initiated and the camera begins to record data. Frames are continuously stored on the 4 gigabyte DRAM internal buffer of the camera while in the capture mode. Once the camera is triggered a pre-set number of frames are saved before and after the trigger time, and the video is downloaded to the camera control software. The software also has a wide variety of image processing tools to adjust brightness, contrast, image orientation, and can determine distances and velocities between frames. The videos can be saved on the computer in a wide array of file formats, in sizes up to the entire buffer of the camera.

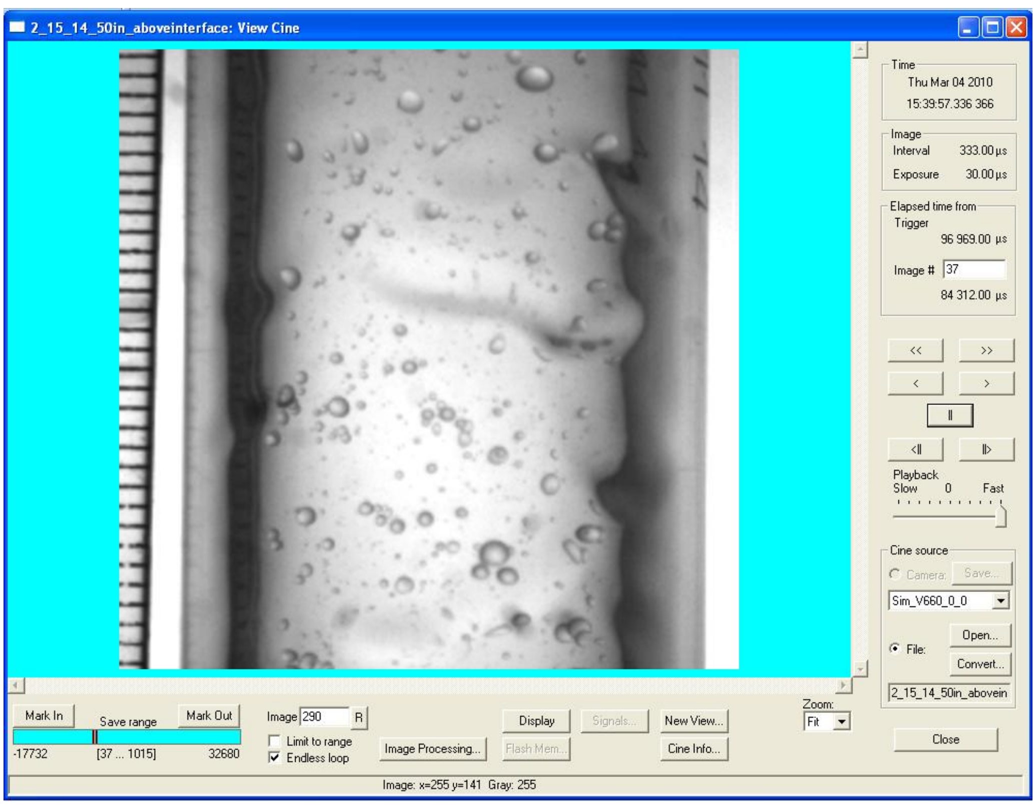

Figure A-7 Screenshot of high speed camera software

The high speed camera requires a standard lens to be attached for adjusting the aperture size and focusing the light onto the sensor array. The lens used for this experiment was a manual focus Nikon 55 mm f3.4 Nikkor lens. It is shown in Figure A-8. The lens used an f-mount and the camera required a c-mount, so an f-mount to c-mount adaptor was required between the lens and the camera. This particular lens had an adjustable aperture with an f# range from 3.4 to 32. A larger f# corresponds to a smaller aperture size and a larger depth of field. This means a longer exposure time is needed to capture enough light, but a deeper range of the subject will be in focus. Equations to calculate the depth of focus for different lens focal length, aperture diameter, and distance from subject can be found in a paper by Ray (1988). These calculations were used to ensure that the entire test section diameter was in focus during visualization.

Figure A-8 High speed camera lens

APPENDIX B

The Engineering Equation Solver code for estimating the oil retained in each test section.

```
$UnitSystem SI, C, MPA

{1.  input parameters}

Psat = 1.157  [MPa]   {specify system saturation pressure in MPa}

w_inlet = 0.05     {speficy OCR}

T_evap_out = 27  {Specify evaporator outlet temperature in C}

m_tot_ho = 12.39/1000    {input total mass retained in kg}
m_tot_vert = 12.30/1000 {input total mass retained in kg}

D= 0.0071                    {Internal Diameter in m}
L_ho = 2.015                {Length in m of horizontal test section}
L_vert = 1.918               {length in m of vertical test section}


{2. determine local oil concentration in liquid}
{2.1  determine two saturation points just above and below Psat}
Pabove = Psat +.005
Pbelow = Psat - .005
Tabove=Temperature(R410A,P=Pabove,x=.1)
Tbelow=Temperature(R410A,P=Pbelow,x=.1)

{2.2 Calculate a_0 and b_0 with w_inlet = 0}
Tabove+273 = a_0 / (ln(Pabove) - b_0)
Tbelow+273 = a_0 / (ln(Pbelow) - b_0)

{2.3 use new values of a_0 and b_0 in equations, keep original values of a_1 to b_4}
a_1 = 182.52
a_2 = -724.21
a_3 = 3868
a_4 = -5268.9

b_1 = -.72212
b_2 = 2.3914
b_3 = -13.779
b_4 = 17.066


{2.4 calculate w_local from T}
A_w_local = a_0 + a_1*w_local + a_2*w_local^3 + a_3*w_local^5 + a_4*w_local^7
B_w_local = b_0 + b_1*w_local + b_2*w_local^3 + b_3*w_local^5 + b_4*w_local^7
T_evap_out+273 = A_w_local / (ln(Psat) - B_w_local)


{3.calculate quality at the inlet of the text section}
w_local= w_inlet / (1-x)

{calculate density of the liquid and vapor portions}
```

```
rho_v=Density(R410A,T=T_evap_out,P=Psat)
rho_r=Density(R410A,T=T_evap_out,x=0)
rho_o =  -1.0127*T_evap_out + 1046.6   {from ASHRAE handbook}
rho_l =rho_o/(1+(1-w_local)*((rho_o/rho_r)-1))  {ideal mixing law}

{Calculate mass of refrigerant vapor, refrigerant liquid, and oil}
V_ho = L_ho*(pi*D^2)/4
V_vert = L_vert*(pi*D^2)/4

m_v_ho+m_l_ho=m_tot_ho
m_v_vert+m_l_vert=m_tot_vert

V_v_ho+V_l_ho=V_ho
V_v_vert+V_l_vert=V_vert

V_v_ho * rho_v = m_v_ho
V_v_vert * rho_v = m_v_vert

V_l_ho * rho_l = m_l_ho
V_l_vert * rho_l = m_l_vert

Alpha_ho = V_v_ho / V_ho
Alpha_vert = V_v_vert / V_vert

m_ref_ho = m_v_ho + (m_l_ho * (1-w_local))
m_ref_vert = m_v_vert + (m_l_vert * (1-w_local))

m_o_ho = m_l_ho * w_local
m_o_vert = m_l_vert  * w_local
```

APPENDIX C

The raw data from the experiments is presented in this appendix. All experiments were taken at a saturation temperature of 12 °C. The experiments are numbered for presentation only, the numbers do not reflect the order in which they were taken. The nominal parameters for each test are shown at the top of each page.

Order:

1. 7.2 mm tube
    a. 5% OCR
        i. 5 °C Apparent Superheat
        ii. 10 °C Apparent Superheat
        iii. 15 °C Apparent Superheat
    b. 3% OCR
        i. 10 °C Apparent Superheat
        ii. 15 °C Apparent Superheat
    c. 1% OCR
        i. 10 °C Apparent Superheat
        ii. 15 °C Apparent Superheat
2. 18.5 mm tube
    a. 5% OCR
        i. 15 °C Apparent Superheat
    b. 3% OCR
        i. 15 °C Apparent Superheat

Units

P_sat	OCR	T_ref_evap_out	T_ref_evap_wall	T_ts_out
kPa	unitless	°C	°C	°C
T_sat	T_ref_evap_in	T_w_e_in	T_w_e_out	
°C	°C	°C	°C	
T_ref_cond_out	T_ref_subcooler_out	T_oil		
°C	°C	°C		
m_ref	m_oil	m_ref_oil	m_water	
g/s	g/s	g/s	g/s	
rho_ref	rho_oil	OMF oil tank		
kg/m^3	kg/m^3	unitless		
dP_refoil_h	dP_refoil_v	dp_refoil_evap		
kPa	kPa	kPa		
dH_refoil	G_mass_flux			
W	kg/m^2s			

Test 1
Pipe: 7.2 mm
OCR: 5%
Apparent Superheat: 5°C
Mass Flux: 100 kg/m^{2}s

P_sat	OCR	T_ref_evap_out	T_ref_evap_wall	T_ts_out
1160	0.0509	17.8	17.8	18.4

T_sat	T_ref_evap_in	T_w_e_in	T_w_e_out
12.3	11.4	18.6	17.9

T_ref_cond_out	T_ref_subcooler_out	T_oil
10.2	10.6	6.4

m_ref	m_oil	m_ref_oil	m_water
3.66	0.40	4.06	265

rho_ref	rho_oil	OMF oil tank
1123.4	1033.9	0.518

dP_refoil_h	dP_refoil_v	dp_refoil_evap
1.95	4.76	0.23

dH_refoil	G_mass_flux
174.9	100.7

Weight Measurement Sheet							Tube weights (g)	
Date	1/20/2010						horizontal	1305
Tester	kurt and ankit						vertical	1248.95
Filename:	omf5_x5_m4_jan2010_1743							
	Sheath Weights full (g)			Final	Sheath weights vented			final
Horizonta	509.41	509.42	509.41	509.4133	509.49	509.48	509.49	509.4867
Vertical	479.59	479.6	479.61	479.6	479.63	479.64	479.65	479.64
	Sheath + Full Tube Weight (g)							
Horizonta	1826.07	1826.07	1826.07				1826.07	
Vertical	1741.72	1741.74	1741.7				1741.72	
	Sheath + Vented Tube Weight (g)							
Horizonta	1820.02	1820.03	1820.02				1820.023	
Vertical	1735.35	1735.35	1735.35				1735.35	
	Measured				Calculated			
	oil	R410a	sum		oil	R410a		error
Horizonta	5.5366667	6.12	11.65667		5.21	6.446667		0.059001
Vertical	6.76	6.41	13.17		6.28	6.89		0.071006

Test 2
Pipe: 7.2 mm
OCR: 5%
Apparent Superheat: 5°C
Mass Flux: 150 kg/m^{2}s

P_sat	OCR	T_ref_evap_out	T_ref_evap_wall	T_ts_out
1155	0.0497	17.7	17.7	17.8

T_sat	T_ref_evap_in	T_w_e_in	T_w_e_out
12.2	10.6	19.3	18.3

T_ref_cond_out	T_ref_subcooler_out	T_oil
10.0	9.9	6.6

m_ref	m_oil	m_ref_oil	m_water
5.39	0.56	5.95	272

rho_ref	rho_oil	OMF oil tank
1127.3	1032.0	0.525

dP_refoil_h	dP_refoil_v	dp_refoil_evap
5.91	7.38	0.32

dH_refoil	G_mass_flux
182.2	147.6

Weight Measurement Sheet
Date 1/19/2010
Tester Kurt and Ankit

Tube weights (g)	
horizontal	1305
vertical	1248.95

Filename: OMF5_x5_m6_Jan1910_1401

	Sheath Weights full (g)			Final	Sheath weights vented			final
Horizonta	509.49	509.48	509.49	509.4867	509.49	509.48	509.47	509.48
Vertical	479.61	479.6	479.6	479.6033	479.55	479.56	479.59	479.5667

	Sheath + Full Tube Weight (g)						
Horizonta	1825.45	1825.44	1825.44				1825.443
Vertical	1740.04	1740.05	1740.04				1740.043

	Sheath + Vented Tube Weight (g)						
Horizonta	1819.66	1819.65	1819.65				1819.653
Vertical	1734.27	1734.26	1734.29				1734.273

	Measured				Calculated			
	oil	R410a	sum		oil	R410a		error
Horizonta	5.1733333	5.783333	10.95667		4.791	6.165667		0.073905
Vertical	5.7566667	5.733333	11.49		5.234	6.256		0.090793

Test 3
Pipe: 7.2 mm
OCR: 5%
Apparent Superheat: 5°C
Mass Flux: 200 kg/m^2s

P_sat	OCR	T_ref_evap_out	T_ref_evap_wall	T_ts_out
1162	0.0512	17.8	17.6	17.0

T_sat	T_ref_evap_in	T_w_e_in	T_w_e_out
12.4	9.4	20.6	19.3

T_ref_cond_out	T_ref_subcooler_out	T_oil
9.4	8.8	6.1

m_ref	m_oil	m_ref_oil	m_water
7.10	0.79	7.89	264

rho_ref	rho_oil	OMF oil tank
1131.9	1035.7	0.511

dP_refoil_h	dP_refoil_v	dp_refoil_evap
11.01	12.49	0.26

dH_refoil	G_mass_flux
191.0	195.7

Weight Measurement Sheet

Date	1/21/2010
Tester	kurt

Tube weights (g)	
horizontal	1305
vertical	1248.95

Filename: omf5_x5_m8_jan2110_1209

	Sheath Weights full (g)			Final	Sheath weights vented			final
Horizonta	509.74	509.73	509.74	509.7367	509.78	509.77	509.78	509.7767
Vertical	479.87	479.88	479.89	479.88	479.94	479.95	479.93	479.94

	Sheath + Full Tube Weight (g)			
Horizonta	1825.42	1825.45	1825.44	1825.437
Vertical	1740.47	1740.42	1740.44	1740.443

	Sheath + Vented Tube Weight (g)			
Horizonta	1819.5	1819.49	1819.5	1819.497
Vertical	1734.66	1734.65	1734.66	1734.657

	Measured			Calculated		
	oil	R410a	sum	oil	R410a	error
Horizonta	4.72	5.98	10.7	4.53	6.17	0.040254
Vertical	5.7666667	5.846667	11.61333	5.21	6.403333	0.096532

Test 4
Pipe: 7.2 mm
OCR: 5%
Apparent Superheat: 10°C
Mass Flux: 100 kg/m^{2}s

P_sat	OCR	T_ref_evap_out	T_ref_evap_wall	T_ts_out
1157	0.0499	22.1	21.8	21.2

T_sat	T_ref_evap_in	T_w_e_in	T_w_e_out
12.2	11.8	22.2	21.6

T_ref_cond_out	T_ref_subcooler_out	T_oil
10.1	10.5	6.1

m_ref	m_oil	m_ref_oil	m_water
3.63	0.45	4.08	282

rho_ref	rho_oil	OMF oil tank
1124.2	1047.2	0.455

dP_refoil_h	dP_refoil_v	dp_refoil_evap
2.67	5.05	0.21

dH_refoil	G_mass_flux
181.2	101.2

Weight Measurement Sheet							Tube weights (g)	
Date	2/2/2010						horizontal	1305
Tester	kurt and ankit						vertical	1248.95
Filename:	omf5_x10_m4_feb0210_1413							
	Sheath Weights full (g)			Final	Sheath weights vented			final
Horizonta	509.09	509.08	509.09	509.0867	509.16	509.17	509.15	509.16
Vertical	479.3	479.31	479.3	479.3033	479.3	479.34	479.32	479.32
	Sheath + Full Tube Weight (g)							
Horizonta	1825.94	1825.96	1825.97				1825.957	
Vertical	1740.26	1740.3	1740.27				1740.277	
	Sheath + Vented Tube Weight (g)							
Horizonta	1820.5	1820.5	1820.52				1820.507	
Vertical	1734.8	1734.81	1734.83				1734.813	
	Measured				Calculated			
	oil	R410a	sum		oil	R410a		error
Horizonta	6.3466667	5.523333	11.87		6.19	5.68		0.024685
Vertical	6.5433333	5.48	12.02333		6.42	5.603333		0.018849

Test 5
Pipe: 7.2 mm
OCR: 5%
Apparent Superheat: 10°C
Mass Flux: 100 kg/m^{2}s

P_sat	OCR	T_ref_evap_out	T_ref_evap_wall	T_ts_out
1154	0.0493	22.1	21.8	21.1

T_sat	T_ref_evap_in	T_w_e_in	T_w_e_out
12.1	11.8	22.2	21.6

T_ref_cond_out	T_ref_subcooler_out	T_oil
10.7	10.5	6.1

m_ref	m_oil	m_ref_oil	m_water
3.62	0.46	4.08	276

rho_ref	rho_oil	OMF oil tank
1124.8	1050.8	0.438

dP_refoil_h	dP_refoil_v	dp_refoil_evap
2.71	5.28	0.26

dH_refoil	G_mass_flux
183.1	101.3

Weight Measurement Sheet							Tube weights (g)	
Date	2/3/2009						horizontal	1305
Tester	kurt and ankit						vertical	1248.95
Filename:	omf5_x10_m4_feb0310_1202							
	Sheath Weights full (g)			Final	Sheath weights vented			final
Horizonta	508.68	508.69	508.7	508.69	508.64	508.65	508.66	508.65
Vertical	478.91	478.89	478.88	478.8933	479.89	478.9	478.88	479.2233
	Sheath + Full Tube Weight (g)							
Horizonta	1825.6	1825.63	1825.6				1825.61	
Vertical	1739.9	1739.91	1739.89				1739.9	
	Sheath + Vented Tube Weight (g)							
Horizonta	1820	1819.99	1820.02				1820.003	
Vertical	1734.25	1734.24	1734.26				1734.25	
	Measured				Calculated			
	oil	R410a	sum		oil	R410a		error
Horizonta	6.3533333	5.566667	11.92		6.25	5.67		0.016264
Vertical	6.0766667	5.98	12.05667		6.47	5.586667		0.064728

Test 6
Pipe: 7.2 mm
OCR: 5%
Apparent Superheat: 10°C
Mass Flux: 100 kg/m^{2}s

P_sat	OCR	T_ref_evap_out	T_ref_evap_wall	T_ts_out
1163	0.0498	21.8	21.5	21.2

T_sat	T_ref_evap_in	T_w_e_in	T_w_e_out
12.4	12.0	22.1	21.1

T_ref_cond_out	T_ref_subcooler_out	T_oil
10.7	11.7	7.6

m_ref	m_oil	m_ref_oil	m_water
3.62	0.44	4.06	175

rho_ref	rho_oil	OMF oil tank
1119.7	1043.8	0.456

dP_refoil_h	dP_refoil_v	dp_refoil_evap
2.41	4.78	0.27

dH_refoil	G_mass_flux
180.7	100.7

Weight Measurement Sheet

Date	2/4/2010
Tester	Kurt and Ankit

Tube weights (g)	
horizontal	1305
vertical	1248.95

Filename: omf5_x10_m4_feb0410_1107

	Sheath Weights full (g)			Final	Sheath weights vented			final
Horizonta	508.86	508.85	508.86	508.8567	508.92	508.96	508.98	508.9533
Vertical	479.05	479.04	479.04	479.0433	479.19	479.15	479.22	479.1867

	Sheath + Full Tube Weight (g)						
Horizonta	1826.63	1826.63	1826.61				1826.623
Vertical	1741.33	1741.33	1741.32				1741.327

	Sheath + Vented Tube Weight (g)						
Horizonta	1820.85	1820.83	1820.86				1820.847
Vertical	1735.49	1735.54	1735.5				1735.51

	Measured				Calculated			
	oil	R410a	sum		oil	R410a		error
Horizonta	6.8933333	5.873333	12.76667		6.745	6.021667		0.021518
Vertical	7.3733333	5.96	13.33333		7.264	6.069333		0.014828

Test 7
Pipe: 7.2 mm
OCR: 5%
Apparent Superheat: 10°C
Mass Flux: 100 kg/m^{2}s

P_sat	OCR	T_ref_evap_out	T_ref_evap_wall	T_ts_out
1157	0.0507	22.1	21.7	20.6

T_sat	T_ref_evap_in	T_w_e_in	T_w_e_out
12.2	11.7	22.2	21.3

T_ref_cond_out	T_ref_subcooler_out	T_oil
10.6	10.2	5.8

m_ref	m_oil	m_ref_oil	m_water
3.70	0.43	4.13	194

rho_ref	rho_oil	OMF oil tank
1125.2	1041.8	0.484

dP_refoil_h	dP_refoil_v	dp_refoil_evap
2.56	5.01	0.27

dH_refoil	G_mass_flux
178.8	102.5

Weight Measurement Sheet							Tube weights (g)	
Date	2/5/2010						horizontal	1305
Tester	Kurt and Ankit						vertical	1248.95
Filename:	OMF5_x10_m4_Feb0510_1042							
	Sheath Weights full (g)			Final	Sheath weights vented			final
Horizonta	509.76	509.76	509.76	509.76	509.69	509.69	509.69	509.69
Vertical	479.85	479.86	479.86	479.8567	479.79	479.79	479.8	479.7933
	Sheath + Full Tube Weight (g)							
Horizonta	1827.14	1827.15	1827.15				1827.147	
Vertical	1741.1	1741.12	1741.11				1741.11	
	Sheath + Vented Tube Weight (g)							
Horizonta	1821.22	1821.23	1821.23				1821.227	
Vertical	1735.35	1735.35	1735.35				1735.35	
	Measured				Calculated			
	oil	R410a	sum		oil	R410a		error
Horizonta	6.5366667	5.85	12.38667		6.552	5.834667		0.002346
Vertical	6.6066667	5.696667	12.30333		6.604	5.699333		0.000404

Test 8
Pipe: 7.2 mm
OCR: 5%
Apparent Superheat: 10°C
Mass Flux: 100 kg/m^{2}s

P_sat	OCR	T_ref_evap_out	T_ref_evap_wall	T_ts_out
1155	0.0489	22.0	21.6	20.5

T_sat	T_ref_evap_in	T_w_e_in	T_w_e_out
12.1	11.5	22.2	21.2

T_ref_cond_out	T_ref_subcooler_out	T_oil
10.5	10.6	6.7

m_ref	m_oil	m_ref_oil	m_water
3.62	0.43	4.05	187

rho_ref	rho_oil	OMF oil tank
1124.4	1045.1	0.460

dP_refoil_h	dP_refoil_v	dp_refoil_evap
2.51	5.05	0.04

dH_refoil	G_mass_flux
194.3	100.5

Weight Measurement Sheet						Tube weights (g)	
Date	1/8/2010					horizontal	1305
Tester	Kurt & Ankit					vertical	1210
Filename:	OMF5_x10_m4_Jan0810_1212						
	Sheath Weights full (g)			Final	Sheath weights vented			final
Horizonta	508.13	508.14	508.14	508.1367	508.15	508.16	508.14	508.15
Vertical	478.58	478.6	478.6	478.5933	478.61	478.61	478.61	478.61
	Sheath + Full Tube Weight (g)							
Horizonta	1825.56	1825.57	1825.57				1825.567	
Vertical	1702.57	1702.58	1702.57				1702.573	
	Sheath + Vented Tube Weight (g)							
Horizonta	1819.93	1819.93	1819.92				1819.927	
Vertical	1696.61	1696.64	1696.61				1696.62	
	Measured				Calculated			
	oil	R410a	sum		oil	R410a		error
Horizonta	6.7766667	5.653333	12.43		6.58	5.85		0.029021
Vertical	8.01	5.97	13.98		7.82	6.16		0.02372

Test 9
Pipe: 7.2 mm
OCR: 5%
Apparent Superheat: 10°C
Mass Flux: 100 kg/m^{2}s

P_sat	OCR	T_ref_evap_out	T_ref_evap_wall	T_ts_out
1153	0.0484	22.1	21.6	19.9

T_sat	T_ref_evap_in	T_w_e_in	T_w_e_out
12.1	10.8	22.2	21.5

T_ref_cond_out	T_ref_subcooler_out	T_oil
10.0	9.8	6.3

m_ref	m_oil	m_ref_oil	m_water
3.66	0.44	4.10	276

rho_ref	rho_oil	OMF oil tank
1127.0	1048.6	0.447

dP_refoil_h	dP_refoil_v	dp_refoil_evap
2.78	5.04	0.02

dH_refoil	G_mass_flux
191.1	101.8

Weight Measurement Sheet							Tube weights (g)	
Date	1/29/2010						horizontal	1305
Tester	kurt and ankit						vertical	1248.95
Filename:	omf5_x10_m4_jan2910_1654							
	Sheath Weights full (g)			Final	Sheath weights vented			final
Horizonta	508.29	508.29	508.31	508.2967	508.3	508.32	508.31	508.31
Vertical	478.45	478.46	478.44	478.45	478.45	478.49	478.49	478.4767
	Sheath + Full Tube Weight (g)							
Horizonta	1825.36	1825.37	1825.36				1825.363	
Vertical	1739.4	1739.39	1739.39				1739.393	
	Sheath + Vented Tube Weight (g)							
Horizonta	1819.54	1819.54	1819.51				1819.53	
Vertical	1733.58	1733.6	1733.57				1733.583	
	Measured				Calculated			
	oil	R410a	sum		oil	R410a		error
Horizonta	6.22	5.846667	12.06667		6.33	5.736667		0.017685
Vertical	6.1566667	5.836667	11.99333		6.39	5.603333		0.037899

Test 10
Pipe: 7.2 mm
OCR: 5%
Apparent Superheat: 10°C
Mass Flux: 150 kg/m^{2}s

P_sat	OCR	T_ref_evap_out	T_ref_evap_wall	T_ts_out
1153	0.0500	22.2	21.8	20.3

T_sat	T_ref_evap_in	T_w_e_in	T_w_e_out
12.1	9.9	22.5	21.1

T_ref_cond_out	T_ref_subcooler_out	T_oil
9.6	9.2	6.2

m_ref	m_oil	m_ref_oil	m_water
5.40	0.69	6.08	198

rho_ref	rho_oil	OMF oil tank
1130.2	1049.4	0.444

dP_refoil_h	dP_refoil_v	dp_refoil_evap
7.34	8.86	-0.07

dH_refoil	G_mass_flux
199.0	151.0

Weight Measurement Sheet
Date 1/11/2010
Tester KURT & ANKIT

Tube weights (g)	
horizontal	1305
vertical	1210

Filename: OMF5_x10_m6_Jan1110_1039

	Sheath Weights full (g)			Final	Sheath weights vented			final
Horizonta	507.93	507.93	507.93	507.93	507.9	507.9	507.9	507.9
Vertical	478.31	478.31	478.31	478.31	478.33	478.33	478.33	478.33

	Sheath + Full Tube Weight (g)						
Horizonta	1823.7	1823.7	1823.69				1823.697
Vertical	1699.58	1699.58	1699.58				1699.58

	Sheath + Vented Tube Weight (g)						
Horizonta	1818.5	1818.5	1818.5				1818.5
Vertical	1694.33	1694.34	1694.33				1694.333

	Measured				Calculated			
	oil	R410a	sum		oil	R410a		error
Horizonta	5.6	5.166667	10.76667		5.4	5.366667		0.035714
Vertical	6.0033333	5.266667	11.27		5.89	5.38		0.018878

Test 11
Pipe: 7.2 mm
OCR: 5%
Apparent Superheat: 10°C
Mass Flux: 200 kg/m^{2}s

P_sat	OCR	T_ref_evap_out	T_ref_evap_wall	T_ts_out
1159	0.0484	22.0	21.7	20.4

T_sat	T_ref_evap_in	T_w_e_in	T_w_e_out
12.3	9.9	22.6	20.8

T_ref_cond_out	T_ref_subcooler_out	T_oil
9.6	9.5	6.9

m_ref	m_oil	m_ref_oil	m_water
7.19	0.84	8.03	213

rho_ref	rho_oil	OMF oil tank
1129.3	1044.5	0.460

dP_refoil_h	dP_refoil_v	dp_refoil_evap
11.91	13.11	0.22

dH_refoil	G_mass_flux
195.0	199.3

Weight Measurement Sheet

Date	1/11/2010	
Tester	kurt	

Tube weights (g)	
horizontal	1305
vertical	1210

Filename: omf5_x10_m8_jan1110_1642

	Sheath Weights full (g)			Final	Sheath weights vented			final
Horizonta	507.87	507.88	507.87	507.8733	507.87	507.87	507.88	507.8733
Vertical	478.4	478.39	478.4	478.3967	478.32	478.36	478.35	478.3433

	Sheath + Full Tube Weight (g)						
Horizonta	1823.4	1823.4	1823.4				1823.4
Vertical	1698.68	1698.7	1698.69				1698.69

	Sheath + Vented Tube Weight (g)						
Horizonta	1818.43	1818.43	1818.41				1818.423
Vertical	1693.96	1693.99	1693.98				1693.977

	Measured				Calculated			
	oil	R410a	sum		oil	R410a		error
Horizonta	5.55	4.976667	10.52667		5.21	5.316667		0.061261
Vertical	5.6333333	4.66	10.29333		5.15	5.143333		0.085799

Test 12
Pipe: 7.2 mm
OCR: 5%
Apparent Superheat: 10°C
Mass Flux: 250 kg/m^2s

P_sat	OCR	T_ref_evap_out	T_ref_evap_wall	T_ts_out
1157	0.0498	22.1	21.7	20.0

T_sat	T_ref_evap_in	T_w_e_in	T_w_e_out
12.2	9.3	22.5	20.8

T_ref_cond_out	T_ref_subcooler_out	T_oil
9.0	9.0	6.7

m_ref	m_oil	m_ref_oil	m_water
9.02	1.11	10.13	265

rho_ref	rho_oil	OMF oil tank
1131.6	1045.6	0.456

dP_refoil_h	dP_refoil_v	dp_refoil_evap
17.63	18.69	0.53

dH_refoil	G_mass_flux
194.8	251.3

Weight Measurement Sheet

Date	1/12/2010						Tube weights (g)	
Tester	Kurt & Ankit						horizontal	1305
							vertical	1210
Filename:	OMF5_x10_m10_Jan1210_1114							
	Sheath Weights full (g)			Final	Sheath weights vented			final
Horizonta	508.01	508.01	508	508.0067	508.07	508.07	508.07	508.07
Vertical	478.49	478.47	478.47	478.4767	478.53	478.52	478.51	478.52
	Sheath + Full Tube Weight (g)							
Horizonta	1822.89	1822.89	1822.87				1822.883	
Vertical	1698.75	1698.77	1698.77				1698.763	
	Sheath + Vented Tube Weight (g)							
Horizonta	1817.76	1817.74	1817.75				1817.75	
Vertical	1694.01	1693.99	1693.98				1693.993	
	Measured				Calculated			
	oil	R410a	sum		oil	R410a		error
Horizonta	4.68	5.196667	9.876667		4.72	5.156667		0.008547
Vertical	5.4733333	4.813333	10.28667		5.14	5.146667		0.060901

Test 13
Pipe: 7.2 mm
OCR: 5%
Apparent Superheat: 15°C
Mass Flux: 100 kg/m^2s

P_sat	OCR	T_ref_evap_out	T_ref_evap_wall	T_ts_out
1163	0.0492	28.2	27.2	24.4

T_sat	T_ref_evap_in	T_w_e_in	T_w_e_out
12.4	12.0	28.2	26.7

T_ref_cond_out	T_ref_subcooler_out	T_oil
12.1	11.0	7.1

m_ref	m_oil	m_ref_oil	m_water
3.76	0.43	4.19	142

rho_ref	rho_oil	OMF oil tank
1125.0	1040.1	0.479

dP_refoil_h	dP_refoil_v	dp_refoil_evap
3.45	4.14	-0.09

dH_refoil	G_mass_flux
207.6	104.0

Weight Measurement Sheet

Date	12/1/2009
Tester	Kurt and Ankit

Tube weights (g)	
horizontal	1305
vertical	1210

Filename: omf5_x15_m4_dec0109_1142.lvm

	Sheath Weights (g)						Final
Horizonta	510.14	510.13	510.13				510.13
Vertical	480.2	480.19	480.16				480.19

	Sheath + Full Tube Weight (g)						
Horizonta	1828.04	1827.97	1827.97				1828
Vertical	1703.13	1703.13					1703.13

	Sheath + Vented Tube Weight (g)						
Horizonta	1822.06	1822.06					1822.06
Vertical	1697.29	1697.29					1697.29

	Measured				Calculated			
	oil	R410a	sum		oil	R410a		error
Horizonta	6.93	5.94	12.87		7.67	5.49		0.106782
Vertical	7.1	5.84	12.94		7.85	5.36		0.105634

Test 14
Pipe: 7.2 mm
OCR: 5%
Apparent Superheat: 15°C
Mass Flux: 150 kg/m^{2}s

P_sat	OCR	T_ref_evap_out	T_ref_evap_wall	T_ts_out
1180	0.0493	28.1	27.2	24.3

T_sat	T_ref_evap_in	T_w_e_in	T_w_e_out
12.9	10.8	28.3	26.3

T_ref_cond_out	T_ref_subcooler_out	T_oil
11.3	9.8	6.7

m_ref	m_oil	m_ref_oil	m_water
5.44	0.69	6.13	139

rho_ref	rho_oil	OMF oil tank
1129.4	1049.1	0.440

dP_refoil_h	dP_refoil_v	dp_refoil_evap
7.85	9.25	-0.09

dH_refoil	G_mass_flux
187.3	152.0

Weight Measurement Sheet

Date	12/4/2009		
Tester	ankit and kurt		

Tube weights (g)	
horizontal	1305
vertical	1210

Filename: omf5_x15_m6_dec0409_1226

	Sheath Weights (g)			Final				
Horizonta	509.05	509.04	509.04	509.0433	509.05	509.04	509.03	509.04
Vertical	479.16	479.18	479.19	479.1767	479.17	479.18	479.16	479.17

	Sheath + Full Tube Weight (g)			
Horizonta	1824.87	1824.86	1824.87	1824.867
Vertical	1700.86	1700.86	1700.85	1700.857

	Sheath + Vented Tube Weight (g)			
Horizonta	1820.06	1820.07	1820.05	1820.06
Vertical	1695.96	1695.96	1695.98	1695.967

	Measured			Calculated		
	oil	R410a	sum	oil	R410a	error
Horizonta	6.02	4.803333	10.82333	5.95	4.873333	0.011628
Vertical	6.7966667	4.883333	11.68	6.75	4.93	0.006866

Test 15
Pipe: 7.2 mm
OCR: 5%
Apparent Superheat: 15°C
Mass Flux: 150 kg/m^{2}s

P_sat	OCR	T_ref_evap_out	T_ref_evap_wall	T_ts_out
1160	0.0498	27.0	26.1	23.8

T_sat	T_ref_evap_in	T_w_e_in	T_w_e_out
12.3	10.9	27.2	25.0

T_ref_cond_out	T_ref_subcooler_out	T_oil
10.8	10.2	7.0

m_ref	m_oil	m_ref_oil	m_water
5.38	0.62	6.00	134

rho_ref	rho_oil	OMF oil tank
1128.0	1039.3	0.484

dP_refoil_h	dP_refoil_v	dp_refoil_evap
7.60	9.32	0.03

dH_refoil	G_mass_flux
202.0	148.8

Weight Measurement Sheet

Date	12/20/2009
Tester	kurt and ankit

Tube weights (g)	
horizontal	1305
vertical	1210

Filename: omf5_x15_m6_dec2009_1303

	Sheath Weights full (g)			Final	Sheath weights vented			final
Horizonta	509.08	509.06	509.08	509.0733	509.16	509.16	509.16	509.16
Vertical	479.53	479.53	479.52	479.5267	479.57	479.57	479.55	479.5633

	Sheath + Full Tube Weight (g)						
Horizonta	1825.54	1825.53	1825.54	1825.55			1825.54
Vertical	1700.87	1700.86	1700.86	1700.86			1700.863

	Sheath + Vented Tube Weight (g)						
Horizonta	1820.76	1820.76	1820.76				1820.76
Vertical	1696.15	1696.15	1696.15				1696.15

	Measured				Calculated			
	oil	R410a	sum		oil	R410a		error
Horizonta	6.60	4.87	11.47		6.45	5.02		0.022727
Vertical	6.59	4.75	11.34		6.47	4.87		0.017713

Test 16
Pipe: 7.2 mm
OCR: 5%
Apparent Superheat: 15°C
Mass Flux: 175 kg/m^{2}s

P_sat	OCR	T_ref_evap_out	T_ref_evap_wall	T_ts_out
1170	0.0492	26.1	25.4	24.1

T_sat	T_ref_evap_in	T_w_e_in	T_w_e_out
12.6	11.0	26.4	24.4

T_ref_cond_out	T_ref_subcooler_out	T_oil
11.1	10.3	7.4

m_ref	m_oil	m_ref_oil	m_water
6.26	0.73	6.99	143

rho_ref	rho_oil	OMF oil tank
1127.1	1040.9	0.472

dP_refoil_h	dP_refoil_v	dp_refoil_evap
9.83	10.41	0.12

dH_refoil	G_mass_flux
176.1	173.5

Weight Measurement Sheet

Date 9/23/2009
Tester Kurt

Tube weights (g)	
horizontal	1305
vertical	1210

Filename: omf5_x15_m7_nov2309_1401.lvm

Sheath Weights (g)							Final
Horizontal							511.16
Vertical							480.99

Sheath + Full Tube Weight (g)							
Horizontal							1827.07
Vertical							1701.62

Sheath + Vented Tube Weight (g)							
Horizontal							1821.95
Vertical							1697.2

	Measured			Calculated		
	oil	R410a	sum	oil	R410a	error
Horizonta	5.79	5.12	10.91	5.88	5.03	0.015544
Vertical	6.21	4.42	10.63	5.78	4.85	0.069243

Test 17
Pipe: 7.2 mm
OCR: 5%
Apparent Superheat: 15°C
Mass Flux: 200 kg/m^2s

P_sat	OCR	T_ref_evap_out	T_ref_evap_wall	T_ts_out
1162	0.0497	27.0	26.1	23.9

T_sat	T_ref_evap_in	T_w_e_in	T_w_e_out
12.4	10.5	27.3	24.9

T_ref_cond_out	T_ref_subcooler_out	T_oil
10.4	10.1	7.3

m_ref	m_oil	m_ref_oil	m_water
6.96	1.01	7.96	140

rho_ref	rho_oil	OMF oil tank
1128.5	1057.0	0.394

dP_refoil_h	dP_refoil_v	dp_refoil_evap
12.92	13.65	0.23

dH_refoil	G_mass_flux
177.0	197.6

Weight Measurement Sheet							Tube weights (g)	
Date	12/21/2009						horizontal	1305
Tester	ankit						vertical	1210
Filename:	OMF5_x15_m8_Dec2109_1218							
	Sheath Weights full (g)			Final	Sheath weights vented			final
Horizonta	509.05	509.05	509.05	509.05	509.06	509.05	509.05	509.0533
Vertical	479.49	479.49	479.48	479.4867	479.49	479.49	479.48	479.4867
	Sheath + Full Tube Weight (g)							
Horizonta	1824.52	1824.53	1824.52				1824.523	
Vertical	1699.92	1699.94	1699.93				1699.93	
	Sheath + Vented Tube Weight (g)							
Horizonta	1819.92	1819.93	1819.93				1819.927	
Vertical	1695.43	1695.42	1695.42				1695.423	
	Measured				Calculated			
	oil	R410a	sum		oil	R410a		error
Horizonta	5.87333333	4.6	10.47333		5.65	4.823333		0.038025
Vertical	5.93666667	4.506667	10.44333		5.73	4.713333		0.034812

Test 18
Pipe: 7.2 mm
OCR: 5%
Apparent Superheat: 15°C
Mass Flux: 250 kg/m^{2}s

P_sat	OCR	T_ref_evap_out	T_ref_evap_wall	T_ts_out
1167	0.0503	29.0	27.9	25.1

T_sat	T_ref_evap_in	T_w_e_in	T_w_e_out
12.5	9.8	29.2	26.5

T_ref_cond_out	T_ref_subcooler_out	T_oil
10.2	9.2	7.0

m_ref	m_oil	m_ref_oil	m_water
8.95	1.08	10.03	186

rho_ref	rho_oil	OMF oil tank
1132.1	1042.4	0.469

dP_refoil_h	dP_refoil_v	dp_refoil_evap
19.07	19.37	0.48

dH_refoil	G_mass_flux
209.5	248.9

Weight Measurement Sheet

Date	12/2/2009
Tester	kurt/ankit

Tube weights (g)	
horizontal	1305
vertical	1210

Filename: omf5_x15_m10_dec0209_1637

	Sheath Weights (g)			for full tube			Final
Horizonta	510.5	510.5	510.5				510.5
Vertical	480.69	480.67	480.69				480.6833
	Sheath + Full Tube Weight (g)						
Horizonta	1826.7	1826.72	1826.72				1826.713
Vertical	1699.34	1699.35	1699.41	1699.41	1699.41	1699.38	1699.383
	Sheath + Vented Tube Weight (g)						
Horizonta	1820.77	1820.76	1820.78				1820.77
Vertical	1694.75	1694.74	1694.73	1694.73			1694.738

	Measured				Calculated			
	oil	R410a	sum		oil	R410a		error
Horizonta	515.77	-504.56	11.21		6.4	4.813333		0.987591
Vertical	484.74	-476.04	8.70		4.51	4.19		0.990696

Test 19
Pipe: 7.2 mm
OCR: 3%
Apparent Superheat: 10°C
Mass Flux: 100 kg/m^{2}s

P_sat	OCR	T_ref_evap_out	T_ref_evap_wall	T_ts_out
1156	0.0300	21.9	21.7	20.9

T_sat	T_ref_evap_in	T_w_e_in	T_w_e_out
12.2	11.3	22.2	21.3

T_ref_cond_out	T_ref_subcooler_out	T_oil
10.3	10.3	6.8

m_ref	m_oil	m_ref_oil	m_water
3.99	0.27	4.25	221

rho_ref	rho_oil	OMF oil tank
1125.6	1041.3	0.476

dP_refoil_h	dP_refoil_v	dp_refoil_evap
2.48	3.87	0.17

dH_refoil	G_mass_flux
192.9	105.6

Weight Measurement Sheet

Date	1/12/2010
Tester	kurt and ankit

Tube weights (g)	
horizontal	1305
vertical	1210

Filename: OMF3_x10_m4_Jan1210_1542

	Sheath Weights full (g)			Final	Sheath weights vented			final
Horizonta	508.14	508.15	508.14	508.1433	508.19	508.2	508.19	508.1933
Vertical	478.56	478.56	478.56	478.56	478.61	478.62	478.63	478.62

	Sheath + Full Tube Weight (g)						
Horizonta	1823.9	1823.93	1823.93				1823.92
Vertical	1700.04	1700.04	1700.04				1700.04

	Sheath + Vented Tube Weight (g)						
Horizonta	1818.79	1818.8	1818.79				1818.793
Vertical	1695.05	1695.05	1695.04				1695.047

	Measured				Calculated			
	oil	R410a	sum		oil	R410a		error
Horizonta	5.6	5.176667	10.77667		5.39	5.386667		0.0375
Vertical	6.42666667	5.053333	11.48		6.02	5.46		0.063278

Test 20
Pipe: 7.2 mm
OCR: 3%
Apparent Superheat: 10°C
Mass Flux: 150 kg/m^{2}s

P_sat	OCR	T_ref_evap_out	T_ref_evap_wall	T_ts_out
1154	0.0309	22.1	21.8	20.6

T_sat	T_ref_evap_in	T_w_e_in	T_w_e_out
12.1	10.3	22.5	21.2

T_ref_cond_out	T_ref_subcooler_out	T_oil
9.6	9.7	6.7

m_ref	m_oil	m_ref_oil	m_water
5.67	0.41	6.08	222

rho_ref	rho_oil	OMF oil tank
1128.8	1044.3	0.463

dP_refoil_h	dP_refoil_v	dp_refoil_evap
6.81	8.17	0.16

dH_refoil	G_mass_flux
206.9	150.8

Weight Measurement Sheet							Tube weights (g)	
Date	1/13/2010						horizontal	1305
Tester	Kurt and Ankit						vertical	1210
Filename:	OMF3_x10_m6_Jan1310_1116							
	Sheath Weights full (g)			Final	Sheath weights vented			final
Horizonta	508.26	508.26	508.26	508.26	508.3	508.3	508.3	508.3
Vertical	478.68	478.71	478.69	478.6933	478.73	478.72	478.74	478.73
	Sheath + Full Tube Weight (g)							
Horizonta	1823.32	1823.33	1823.32				1823.323	
Vertical	1698.95	1698.95	1698.96				1698.953	
	Sheath + Vented Tube Weight (g)							
Horizonta	1818.26	1818.25	1818.25				1818.253	
Vertical	1694.3	1694.3	1694.28				1694.293	
	Measured				Calculated			
	oil	R410a	sum		oil	R410a		error
Horizonta	4.95333333	5.11	10.06333		4.88	5.183333		0.014805
Vertical	5.56333333	4.696667	10.26		5.15	5.11		0.074296

Test 21
Pipe: 7.2 mm
OCR: 3%
Apparent Superheat: 10°C
Mass Flux: 200 kg/m^{2}s

P_sat	OCR	T_ref_evap_out	T_ref_evap_wall	T_ts_out
1158	0.0298	22.2	21.9	20.5

T_sat	T_ref_evap_in	T_w_e_in	T_w_e_out
12.2	9.7	23.0	21.2

T_ref_cond_out	T_ref_subcooler_out	T_oil
9.6	9.2	6.5

m_ref	m_oil	m_ref_oil	m_water
7.44	0.56	8.00	227

rho_ref	rho_oil	OMF oil tank
1130.7	1052.6	0.425

dP_refoil_h	dP_refoil_v	dp_refoil_evap
11.01	12.10	0.29

dH_refoil	G_mass_flux
213.9	198.5

Weight Measurement Sheet							Tube weights (g)	
Date	1/14/2010						horizontal	1305
Tester	kurt and ankit						vertical	1210
Filename:	OMF3_x10_m8_Jan1410_1127							
	Sheath Weights full (g)			Final	Sheath weights vented			final
Horizonta	508.76	508.76	508.76	508.76	508.82	508.82	508.8	508.8133
Vertical	479.21	479.2	479.21	479.2067	479.26	479.26	479.26	479.26
	Sheath + Full Tube Weight (g)							
Horizonta	1822.62	1822.62	1822.61				1822.617	
Vertical	1698.24	1698.24	1698.25				1698.243	
	Sheath + Vented Tube Weight (g)							
Horizonta	1817.99	1817.98	1817.98				1817.983	
Vertical	1693.81	1693.82	1693.82				1693.817	
	Measured				Calculated			
	oil	R410a	sum		oil	R410a		error
Horizonta	4.17	4.686667	8.856667		4.02	4.836667		0.035971
Vertical	4.55666667	4.48	9.036667		4.27	4.766667		0.062911

Test 22
Pipe: 7.2 mm
OCR: 3%
Apparent Superheat: 10°C
Mass Flux: 250 kg/m^{2}s

P_sat	OCR	T_ref_evap_out	T_ref_evap_wall	T_ts_out
1157	0.0295	22.3	21.9	20.2

T_sat	T_ref_evap_in	T_w_e_in	T_w_e_out
12.2	9.4	22.7	21.0

T_ref_cond_out	T_ref_subcooler_out	T_oil
8.8	9.0	6.7

m_ref	m_oil	m_ref_oil	m_water
9.44	0.66	10.10	281

rho_ref	rho_oil	OMF oil tank
1131.6	1046.3	0.453

dP_refoil_h	dP_refoil_v	dp_refoil_evap
16.95	17.74	0.71

dH_refoil	G_mass_flux
205.9	250.6

Weight Measurement Sheet

Date 1/14/2009

Tester kurt and ankit

Tube weights (g)	
horizontal	1305
vertical	1210

Filename: OMF3_x10_m10_Jan1410_1614

	Sheath Weights full (g)			Final	Sheath weights vented			final
Horizonta	508.99	508.98	508.99	508.9867	509.05	509.04	509.07	509.0533
Vertical	479.42	479.42	479.42	479.42	479.19	479.2	479.21	479.2

	Sheath + Full Tube Weight (g)						
Horizonta	1822.02	1822	1822.04				1822.02
Vertical	1697.56	1697.54	1697.52				1697.54

	Sheath + Vented Tube Weight (g)						
Horizonta	1817.85	1817.85	1817.83				1817.843
Vertical	1693.27	1693.26	1693.28				1693.27

	Measured				Calculated			
	oil	R410a	sum		oil	R410a		error
Horizonta	3.79	4.243333	8.033333		3.42	4.613333		0.097625
Vertical	4.07	4.05	8.12		3.6	4.52		0.115479

Test 23
Pipe: 7.2 mm
OCR: 3%
Apparent Superheat: 15°C
Mass Flux: 100 kg/m^{2}s

P_sat	OCR	T_ref_evap_out	T_ref_evap_wall	T_ts_out
1150	0.0289	27.1	26.0	22.9

T_sat	T_ref_evap_in	T_w_e_in	T_w_e_out
12.0	11.0	27.1	25.7

T_ref_cond_out	T_ref_subcooler_out	T_oil
10.5	10.0	6.2

m_ref	m_oil	m_ref_oil	m_water
3.87	0.27	4.14	166

rho_ref	rho_oil	OMF oil tank
1127.5	1049.3	0.445

dP_refoil_h	dP_refoil_v	dp_refoil_evap
2.78	3.99	0.04

dH_refoil	G_mass_flux
224.4	102.7

Weight Measurement Sheet							Tube weights (g)	
Date	1/2/2010						horizontal	1305
Tester	KURT & ANKIT						vertical	1210
Filename:	OMF3_x15_m4_Jan0210_1446							
	Sheath Weights full (g)			Final	Sheath weights vented			final
Horizonta	507.83	507.83	507.83	507.83	507.82	507.82	507.82	507.82
Vertical	478.21	478.21	478.2	478.2067	478.2	478.19	478.2	478.1967
	Sheath + Full Tube Weight (g)							
Horizonta	1822.71	1822.73	1822.71				1822.717	
Vertical	1698.77	1698.77	1698.75				1698.763	
	Sheath + Vented Tube Weight (g)							
Horizonta	1818	1818.01	1818				1818.003	
Vertical	1694.03	1694.05	1694.03				1694.037	
	Measured				Calculated			
	oil	R410a	sum		oil	R410a		error
Horizonta	5.18333333	4.703333	9.886667		5.25	4.636667		0.012862
Vertical	5.84	4.716667	10.55667		5.9	4.656667		0.010274

Test 24
Pipe: 7.2 mm
OCR: 3%
Apparent Superheat: 15°C
Mass Flux: 150 kg/m^{2}s

P_sat	OCR	T_ref_evap_out	T_ref_evap_wall	T_ts_out
1152	0.0292	26.8	26.0	23.6

T_sat	T_ref_evap_in	T_w_e_in	T_w_e_out
12.1	9.9	26.9	25.0

T_ref_cond_out	T_ref_subcooler_out	T_oil
10.1	9.2	6.1

m_ref	m_oil	m_ref_oil	m_water
5.72	0.40	6.12	170

rho_ref	rho_oil	OMF oil tank
1130.9	1048.1	0.451

dP_refoil_h	dP_refoil_v	dp_refoil_evap
7.55	8.77	-0.03

dH_refoil	G_mass_flux
219.3	151.9

Weight Measurement Sheet

		Tube weights (g)	
Date	31/12/09	horizontal	1305
Tester	Kurt and Ankit	vertical	1210

Filename: OMF3_x15_m6_Dec3109_1043

	Sheath Weights full (g)			Final	Sheath weights vented			final
Horizonta	509.48	509.48	509.47	509.4767	509.43	509.43	509.43	509.43
Vertical	479.87	479.85	479.86	479.86	479.78	479.77	479.77	479.7733

	Sheath + Full Tube Weight (g)						
Horizonta	1823.8	1823.8	1823.79				1823.797
Vertical	1699.14	1699.14	1699.12				1699.133

	Sheath + Vented Tube Weight (g)						
Horizonta	1819.06	1819.07	1819.05				1819.06
Vertical	1694.62	1694.62	1694.61				1694.617

	Measured				Calculated			
	oil	R410a	sum		oil	R410a		error
Horizonta	4.63	4.69	9.32		4.79	4.53		0.034557
Vertical	4.84333333	4.43	9.273333		4.88	4.393333		0.007571

Test 25
Pipe: 7.2 mm
OCR: 3%
Apparent Superheat: 15°C
Mass Flux: 200 kg/m^{2}s

P_sat	OCR	T_ref_evap_out	T_ref_evap_wall	T_ts_out
1152	0.0301	27.0	26.2	23.9

T_sat	T_ref_evap_in	T_w_e_in	T_w_e_out
12.1	10.4	27.4	24.6

T_ref_cond_out	T_ref_subcooler_out	T_oil
10.2	10.0	7.6

m_ref	m_oil	m_ref_oil	m_water
7.47	0.53	8.00	149

rho_ref	rho_oil	OMF oil tank
1128.8	1044.1	0.454

dP_refoil_h	dP_refoil_v	dp_refoil_evap
12.44	12.87	0.32

dH_refoil	G_mass_flux
216.7	198.5

Weight Measurement Sheet						Tube weights (g)	
Date	12/22/2009					horizontal	1305
Tester	Kurt and Ankit					vertical	1210
Filename:	omf3_x15_m8_dec2209_1304.lvm						
	Sheath Weights full (g)			Final	Sheath weights vented		final
Horizonta	509.31	509.3	509.31	509.3067	509.31	509.3	509.28	509.2967
Vertical	479.68	479.71	479.7	479.6967	479.68	479.68	479.68	479.68

	Sheath + Full Tube Weight (g)						
Horizonta	1823.2	1823.2	1823.2				1823.2
Vertical	1698.48	1698.48	1698.49				1698.483
	Sheath + Vented Tube Weight (g)						
Horizonta	1818.68	1818.68	1818.68				1818.68
Vertical	1694.38	1694.38	1694.38				1694.38

	Measured				Calculated			
	oil	R410a	sum		oil	R410a		error
Horizonta	4.38333333	4.51	8.893333		4.47	4.423333		0.019772
Vertical	4.7	4.086667	8.786667		4.51	4.276667		0.040426

Test 26
Pipe: 7.2 mm
OCR: 3%
Apparent Superheat: 15°C
Mass Flux: 250 kg/m^2s

P_sat	OCR	T_ref_evap_out	T_ref_evap_wall	T_ts_out
1158	0.0311	27.0	26.1	23.4

T_sat	T_ref_evap_in	T_w_e_in	T_w_e_out
12.3	9.2	27.3	24.3

T_ref_cond_out	T_ref_subcooler_out	T_oil
9.2	8.9	6.5

m_ref	m_oil	m_ref_oil	m_water
9.21	0.93	10.14	170

rho_ref	rho_oil	OMF oil tank
1132.4	1070.2	0.342

dP_refoil_h	dP_refoil_v	dp_refoil_evap
18.26	18.53	0.47

dH_refoil	G_mass_flux
217.4	251.6

Weight Measurement Sheet								Tube weights (g)	
Date	1/1/2010							horizontal	1305
Tester	Kurt and Ankit							vertical	1210
									4
Filename:	OMF3_x15_m10_Jan0110_1254								
	Sheath Weights full (g)			Final	Sheath weights vented			final	
Horizonta	508.34	508.34	508.34	508.34	508.28	508.28	508.28	508.28	
Vertical	478.69	478.69	478.68	478.6867	478.68	478.68	478.68	478.68	
	Sheath + Full Tube Weight (g)								
Horizonta	1821.99	1822	1821.98				1821.99		
Vertical	1696.51	1696.51	1696.48				1696.5		
	Sheath + Vented Tube Weight (g)								
Horizonta	1817.41	1817.43	1817.41				1817.417		
Vertical	1692.56	1692.56	1692.56				1692.56		
	Measured				Calculated				
	oil	R410a	sum		oil	R410a		error	
Horizonta	4.13666667	4.513333	8.65		4.24	4.41		0.02498	
Vertical	3.88	3.933333	7.813333		3.71	4.103333		0.043814	

Test 27
Pipe: 7.2 mm
OCR: 1%
Apparent Superheat: 10°C
Mass Flux: 100 kg/m^{2}s

P_sat	OCR	T_ref_evap_out	T_ref_evap_wall	T_ts_out
1155	0.0105	22.2	22.0	21.0

T_sat	T_ref_evap_in	T_w_e_in	T_w_e_out
12.1	11.1	22.3	21.6

T_ref_cond_out	T_ref_subcooler_out	T_oil
10.2	10.5	9.0

m_ref	m_oil	m_ref_oil	m_water
4.00	0.10	4.10	291

rho_ref	rho_oil	OMF oil tank
1124.5	1041.5	0.450

dP_refoil_h	dP_refoil_v	dp_refoil_evap
1.57	2.54	0.19

dH_refoil	G_mass_flux
205.8	101.7

Weight Measurement Sheet							Tube weights (g)	
Date	1/15/2010						horizontal	1305
Tester	Kurt and Ankit						vertical	1210
Filename:	OMF1_x10_m4_Jan1510_1052							
	Sheath Weights full (g)			Final	Sheath weights vented			final
Horizonta	509.18	509.19	509.19	509.1867	509.19	509.2	509.19	509.1933
Vertical	479.41	479.4	479.41	479.4067	479.32	479.33	479.32	479.3233
	Sheath + Full Tube Weight (g)							
Horizonta	1822.4	1822.39	1822.39				1822.393	
Vertical	1699.98	1700	1699.98				1699.987	
	Sheath + Vented Tube Weight (g)							
Horizonta	1817.68	1817.71	1817.69				1817.693	
Vertical	1694.83	1694.83	1694.82				1694.827	
	Measured				Calculated			
	oil	R410a	sum		oil	R410a		error
Horizonta	3.5	4.706667	8.206667		3.56	4.646667		0.017143
Vertical	5.50333333	5.076667	10.58		5.4	5.18		0.018776

Test 28
Pipe: 7.2 mm
OCR: 1%
Apparent Superheat: 10°C
Mass Flux: 100 kg/m^2s

P_sat	OCR	T_ref_evap_out	T_ref_evap_wall	T_ts_out
1160	0.0113	22.1	21.9	21.1

T_sat	T_ref_evap_in	T_w_e_in	T_w_e_out
12.3	10.9	22.3	21.5

T_ref_cond_out	T_ref_subcooler_out	T_oil
10.7	9.9	8.3

m_ref	m_oil	m_ref_oil	m_water
4.05	0.11	4.15	279

rho_ref	rho_oil	OMF oil tank
1127.7	1045.4	0.439

dP_refoil_h	dP_refoil_v	dp_refoil_evap
1.60	3.18	0.18

dH_refoil	G_mass_flux
202.0	103.1

Weight Measurement Sheet

Date	1/18/2010
Tester	Kurt and Ankit

Tube weights (g)	
horizontal	1305
vertical	1248.95

Filename: OMF1_x10_m4_Jan1810_1224

	Sheath Weights full (g)			Final	Sheath weights vented			final
Horizonta	509.54	509.54	509.53	509.5367	509.58	509.58	509.56	509.5733
Vertical	479.6	479.61	479.62	479.61	479.68	479.68	479.68	479.68

	Sheath + Full Tube Weight (g)						
Horizonta	1822.57	1822.58	1822.56				1822.57
Vertical	1737.6	1737.6	1737.59				1737.597

	Sheath + Vented Tube Weight (g)						
Horizonta	1818.12	1818.11	1818.11				1818.113
Vertical	1732.14	1732.92	1732.93				1732.663

	Measured				Calculated			
	oil	R410a	sum		oil	R410a		error
Horizonta	3.54	4.493333	8.033333		3.39	4.643333		0.042373
Vertical	4.03333333	5.003333	9.036667		4.24	4.796667		0.05124

Test 29
Pipe: 7.2 mm
OCR: 1%
Apparent Superheat: 10°C
Mass Flux: 150 kg/m^{2}s

P_sat	OCR	T_ref_evap_out	T_ref_evap_wall	T_ts_out
1169	0.0092	22.2	22.1	20.8

T_sat	T_ref_evap_in	T_w_e_in	T_w_e_out
12.6	10.0	24.2	22.7

T_ref_cond_out	T_ref_subcooler_out	T_oil
10.2	9.3	8.0

m_ref	m_oil	m_ref_oil	m_water
6.00	0.13	6.12	214

rho_ref	rho_oil	OMF oil tank
1129.3	1046.0	0.440

dP_refoil_h	dP_refoil_v	dp_refoil_evap
4.50	5.32	0.19

dH_refoil	G_mass_flux
217.1	152.0

Weight Measurement Sheet

Date	1/16/2010
Tester	kurt

Tube weights (g)	
horizontal	1305
vertical	1210

Filename: OMF1_x10_m6_Jan1610_1434

	Sheath Weights full (g)			Final	Sheath weights vented			final
Horizonta	509.33	509.29	509.29	509.3033	509.35	509.35	509.37	509.3567
Vertical	479.48	479.48	479.46	479.4733	479.46	479.47	479.48	479.47

	Sheath + Full Tube Weight (g)						
Horizonta	1822.39	1822.4	1822.4				1822.397
Vertical	1697.01	1696.97	1696.98	1696.97			1696.983

	Sheath + Vented Tube Weight (g)						
Horizonta	1817.7	1817.81	1817.7				1817.737
Vertical	1692.69	1692.7	1692.69				1692.693

	Measured				Calculated			
	oil	R410a	sum		oil	R410a		error
Horizonta	3.38	4.713333	8.093333		3.41	4.683333		0.008876
Vertical	3.22333333	4.285833	7.509167		3.11	4.399167		0.03516

Test 30
Pipe: 7.2 mm
OCR: 1%
Apparent Superheat: 10°C
Mass Flux: 150 kg/m^{2}s

P_sat	OCR	T_ref_evap_out	T_ref_evap_wall	T_ts_out
1161	0.0114	22.2	22.0	21.1

T_sat	T_ref_evap_in	T_w_e_in	T_w_e_out
12.3	9.9	22.4	21.3

T_ref_cond_out	T_ref_subcooler_out	T_oil
9.6	9.2	7.5

m_ref	m_oil	m_ref_oil	m_water
6.15	0.16	6.30	285

rho_ref	rho_oil	OMF oil tank
1130.2	1043.1	0.459

dP_refoil_h	dP_refoil_v	dp_refoil_evap
5.17	6.14	0.23

dH_refoil	G_mass_flux
209.3	156.4

Weight Measurement Sheet							Tube weights (g)	
Date	1/17/2010						horizontal	1305
Tester	kurt and ankit						vertical	1210
								3
Filename:	OMF1_x10_m6_Jan1710_1530							
	Sheath Weights full (g)			Final	Sheath weights vented			final
Horizonta	509.31	509.31	509.3	509.3067	509.34	509.31	509.31	509.32
Vertical	479.42	479.42	479.4	479.4133	479.42	479.41	479.43	479.42
	Sheath + Full Tube Weight (g)							
Horizonta	1822.5	1822.5	1822.48				1822.493	
Vertical	1697.3	1697.32	1697.29				1697.303	
	Sheath + Vented Tube Weight (g)							
Horizonta	1818.05	1818.05	1818.04				1818.047	
Vertical	1693.08	1693.07	1693.07				1693.073	
	Measured				Calculated			
	oil	R410a	sum		oil	R410a		error
Horizonta	3.73	4.46	8.186667		3.52	4.666667		0.055456
Vertical	3.65	4.236667	7.89		3.42	4.47		0.063869

Test 31
Pipe: 7.2 mm
OCR: 1%
Apparent Superheat: 10°C
Mass Flux: 200 kg/m^{2}s

P_sat	OCR	T_ref_evap_out	T_ref_evap_wall	T_ts_out
1157	0.0110	22.4	22.2	21.1

T_sat	T_ref_evap_in	T_w_e_in	T_w_e_out
12.2	9.4	22.8	21.4

T_ref_cond_out	T_ref_subcooler_out	T_oil
9.4	9.0	7.1

m_ref	m_oil	m_ref_oil	m_water
7.97	0.19	8.16	292

rho_ref	rho_oil	OMF oil tank
1130.8	1043.7	0.461

dP_refoil_h	dP_refoil_v	dp_refoil_evap
9.09	9.93	0.47

dH_refoil	G_mass_flux
209.5	202.6

Weight Measurement Sheet

Date	1/16/2010					Tube weights (g)	
Tester	Kurt and Ankit					horizontal	1305
						vertical	1210
Filename:	OMF1_x10_m8_Jan1610_1822						
	Sheath Weights full (g)			Final	Sheath weights vented		final
Horizonta	509.42	509.41	509.38	509.4033	509.37	509.4	509.37	509.38
Vertical	479.51	479.52	479.51	479.5133	479.48	479.51	479.51	479.5
	Sheath + Full Tube Weight (g)							
Horizonta	1821.63	1821.62	1821.6				1821.617	
Vertical	1696.82	1696.82	1696.79				1696.81	
	Sheath + Vented Tube Weight (g)							
Horizonta	1817.34	1817.33	1817.33				1817.333	
Vertical	1692.63	1692.66	1692.66				1692.65	
	Measured				Calculated			
	oil	R410a	sum		oil	R410a		error
Horizonta	2.95333333	4.26	7.213333		2.84	4.373333		0.038375
Vertical	3.15	4.146667	7.296667		3.02	4.276667		0.04127

Test 32
Pipe: 7.2 mm
OCR: 1%
Apparent Superheat: 10°C
Mass Flux: 250 kg/m^{2}s

P_sat	OCR	T_ref_evap_out	T_ref_evap_wall	T_ts_out
1161	0.0107	22.4	22.2	20.6

T_sat	T_ref_evap_in	T_w_e_in	T_w_e_out
12.3	8.8	23.5	21.6

T_ref_cond_out	T_ref_subcooler_out	T_oil
9.2	8.5	6.8

m_ref	m_oil	m_ref_oil	m_water
9.81	0.23	10.04	284

rho_ref	rho_oil	OMF oil tank
1133.4	1044.1	0.462

dP_refoil_h	dP_refoil_v	dp_refoil_evap
13.53	14.19	0.70

dH_refoil	G_mass_flux
216.6	249.2

Weight Measurement Sheet							Tube weights (g)	
Date	1/17/2010						horizontal	1305
Tester	kurt and ankit						vertical	1210
Filename:	OMF1_x10_m10_Jan1710_1101							
	Sheath Weights full (g)			Final	Sheath weights vented			final
Horizonta	509.41	509.4	509.39	509.4	509.34	509.35	509.34	509.3433
Vertical	479.5	479.5	479.51	479.5033	479.45	479.45	479.45	479.45
	Sheath + Full Tube Weight (g)							
Horizonta	1821.18	1821.18	1821.18				1821.18	
Vertical	1697.15	1697.14	1697.11				1697.133	
	Sheath + Vented Tube Weight (g)							
Horizonta	1817.03	1817.05	1817.04				1817.04	
Vertical	1692.91	1692.92	1692.9				1692.91	
	Measured				Calculated			
	oil	R410a	sum		oil	R410a		error
Horizonta	2.69666667	4.083333	6.78		2.51	4.27		0.069221
Vertical	3.46	4.17	7.63		3.25	4.38		0.060694

Test 33
Pipe: 7.2 mm
OCR: 1%
Apparent Superheat: 15°C
Mass Flux: 100 kg/m^{2}s

P_sat	OCR	T_ref_evap_out	T_ref_evap_wall	T_ts_out
1158	0.0098	27.1	26.2	23.0

T_sat	T_ref_evap_in	T_w_e_in	T_w_e_out
12.2	11.5	27.1	25.8

T_ref_cond_out	T_ref_subcooler_out	T_oil
10.8	10.7	9.3

m_ref	m_oil	m_ref_oil	m_water
4.11	0.10	4.21	159

rho_ref	rho_oil	OMF oil tank
1124.4	1050.2	0.403

dP_refoil_h	dP_refoil_v	dp_refoil_evap
1.73	2.65	0.15

dH_refoil	G_mass_flux
216.4	104.4

Weight Measurement Sheet

Date	1/7/2010		
Tester	Kurt and Ankit		
Filename:	OMF1_x15_m4_Jan0710_1031		

Tube weights (g)	
horizontal	1305
vertical	1210

	Sheath Weights full (g)			Final	Sheath weights vented			final
Horizonta	508.15	508.15	508.15	508.15	508.14	508.14	508.14	508.14
Vertical	478.61	478.6	478.6	478.6033	478.58	478.58	478.58	478.58

	Sheath + Full Tube Weight (g)						
Horizonta	1820.58	1820.59	1820.59				1820.587
Vertical	1697.61	1697.61	1697.59				1697.603

	Sheath + Vented Tube Weight (g)						
Horizonta	1816.4	1816.4	1816.4				1816.4
Vertical	1693.11	1693.12	1693.12				1693.117

	Measured				Calculated			
	oil	R410a	sum		oil	R410a		error
Horizonta	3.26	4.176667	7.436667		3.28	4.156667		0.006135
Vertical	4.53666667	4.463333	9		4.64	4.36		0.022777

Test 34
Pipe: 7.2 mm
OCR: 1%
Apparent Superheat: 15°C
Mass Flux: 150 kg/m^{2}s

P_sat	OCR	T_ref_evap_out	T_ref_evap_wall	T_ts_out
1155	0.0101	27.2	26.3	23.3

T_sat	T_ref_evap_in	T_w_e_in	T_w_e_out
12.2	10.6	27.4	25.3

T_ref_cond_out	T_ref_subcooler_out	T_oil
10.2	10.1	8.5

m_ref	m_oil	m_ref_oil	m_water
5.83	0.15	5.98	158

rho_ref	rho_oil	OMF oil tank
1127.0	1054.0	0.394

dP_refoil_h	dP_refoil_v	dp_refoil_evap
4.86	5.43	0.08

dH_refoil	G_mass_flux
229.3	148.4

Weight Measurement Sheet

Date	1/4/2010
Tester	KURT and ANKIT

Tube weights (g)	
horizontal	1305
vertical	1210

Filename: omf1_x15_m6_jan0210_1440

	Sheath Weights full (g)			Final	Sheath weights vented			final
Horizonta	507.6	507.57	507.57	507.58	507.59	507.59	507.57	507.5833
Vertical	478.05	478.05	478.02	478.04	478.03	478.01	478.02	478.02

	Sheath + Full Tube Weight (g)						
Horizonta	1821.15	1821.17	1821.14				1821.153
Vertical	1695.48	1695.46	1695.46				1695.467

	Sheath + Vented Tube Weight (g)						
Horizonta	1816.62	1816.62	1816.62				1816.62
Vertical	1691.44	1691.44	1691.43				1691.437

	Measured				Calculated			
	oil	R410a	sum		oil	R410a		error
Horizonta	4.03666667	4.536667	8.573333		4.21	4.363333		0.04294
Vertical	3.41666667	4.01	7.426667		3.44	3.986667		0.006829

Test 35
Pipe: 7.2 mm
OCR: 1%
Apparent Superheat: 15°C
Mass Flux: 150 kg/m^{2}s

P_sat	OCR	T_ref_evap_out	T_ref_evap_wall	T_ts_out
1157	0.0105	27.1	26.2	23.3

T_sat	T_ref_evap_in	T_w_e_in	T_w_e_out
12.2	10.5	27.2	25.2

T_ref_cond_out	T_ref_subcooler_out	T_oil
10.1	9.9	8.3

m_ref	m_oil	m_ref_oil	m_water
6.00	0.16	6.17	168

rho_ref	rho_oil	OMF oil tank
1127.2	1054.5	0.394

dP_refoil_h	dP_refoil_v	dp_refoil_evap
5.38	6.22	0.17

dH_refoil	G_mass_flux
231.0	153.0

Weight Measurement Sheet

Date	1/7/2010	Tube weights (g)	
Tester	KURT & ANKIT	horizontal	1305
		vertical	1210

Filename: OMF1_x15_m6_Jan0710_1516

	Sheath Weights full (g)			Final	Sheath weights vented			final
Horizonta	508.17	508.17	508.17	508.17	508.14	508.15	508.14	508.1433
Vertical	478.61	478.61	478.61	478.61	478.56	478.58	478.57	478.57

	Sheath + Full Tube Weight (g)			
Horizonta	1820.79	1820.79	1820.79	1820.79
Vertical	1696.72	1696.73	1696.7	1696.717

	Sheath + Vented Tube Weight (g)			
Horizonta	1816.66	1816.67	1816.66	1816.663
Vertical	1692.6	1692.59	1692.61	1692.6

	Measured			Calculated		
	oil	R410a	sum	oil	R410a	error
Horizonta	3.52	4.1	7.62	3.43	4.19	0.025568
Vertical	4.03	4.076667	8.106667	3.93	4.176667	0.024814

Test 36
Pipe: 7.2 mm
OCR: 1%
Apparent Superheat: 15°C
Mass Flux: 200 kg/m^2s

P_sat	OCR	T_ref_evap_out	T_ref_evap_wall	T_ts_out
1158	0.0098	27.1	26.3	23.6

T_sat	T_ref_evap_in	T_w_e_in	T_w_e_out
12.2	9.7	27.5	24.8

T_ref_cond_out	T_ref_subcooler_out	T_oil
9.9	9.4	8.0

m_ref	m_oil	m_ref_oil	m_water
8.03	0.19	8.22	167

rho_ref	rho_oil	OMF oil tank
1130.0	1049.3	0.424

dP_refoil_h	dP_refoil_v	dp_refoil_evap
9.55	9.75	0.27

dH_refoil	G_mass_flux
230.5	204.0

Weight Measurement Sheet
Date 1/5/2010
Tester Kurt and Ankit

Tube weights (g)	
horizontal	1305
vertical	1210

Filename: OMF1_x15_m8_Jan0510_1254

	Sheath Weights full (g)			Final	Sheath weights vented			final
Horizonta	507.58	507.56	507.55	507.5633	507.56	507.55	507.55	507.5533
Vertical	477.97	477.96	477.96	477.9633	477.99	477.98	477.98	477.9833

	Sheath + Full Tube Weight (g)						
Horizonta	1819.63	1819.65	1819.64				1819.64
Vertical	1695.14	1695.15	1695.15				1695.147

	Sheath + Vented Tube Weight (g)						
Horizonta	1815.48	1815.48	1815.46				1815.473
Vertical	1691.29	1691.29	1691.29				1691.29

	Measured				Calculated			
	oil	R410a	sum		oil	R410a		error
Horizonta	2.92	4.156667	7.076667		3.02	4.056667		0.034247
Vertical	3.30666667	3.876667	7.183333		3.23	3.953333		0.023185

Test 37
Pipe: 7.2 mm
OCR: 1%
Apparent Superheat: 15°C
Mass Flux: 250 kg/m^{2}s

P_sat	OCR	T_ref_evap_out	T_ref_evap_wall	T_ts_out
1160	0.0109	27.0	26.2	23.5

T_sat	T_ref_evap_in	T_w_e_in	T_w_e_out
12.3	9.4	27.7	24.5

T_ref_cond_out	T_ref_subcooler_out	T_oil
9.6	9.2	7.4

m_ref	m_oil	m_ref_oil	m_water
9.68	0.29	9.97	171

rho_ref	rho_oil	OMF oil tank
1130.4	1061.9	0.370

dP_refoil_h	dP_refoil_v	dp_refoil_evap
14.49	14.46	0.57

dH_refoil	G_mass_flux
228.4	247.5

Weight Measurement Sheet							Tube weights (g)	
Date	1/6/2010						horizontal	1305
Tester	Kurt and Ankit						vertical	1210
								2.77
Filename:	OMF1_x15_m10_Jan0610_1152							
	Sheath Weights full (g)			Final	Sheath weights vented			final
Horizonta	507.54	507.53	507.53	507.5333	507.57	507.56	507.57	507.5667
Vertical	477.98	477.98	477.97	477.9767	478.02	478.01	478.02	478.0167
	Sheath + Full Tube Weight (g)							
Horizonta	1819.3	1819.32	1819.3				1819.307	
Vertical	1694.16	1694.16	1694.15				1694.157	
	Sheath + Vented Tube Weight (g)							
Horizonta	1815.22	1815.21	1815.21				1815.213	
Vertical	1690.57	1690.57	1690.57				1690.57	
	Measured				Calculated			
	oil	R410a	sum		oil	R410a		error
Horizonta	2.64666667	4.126667	6.773333		2.77	4.003333		0.046599
Vertical	2.55333333	3.626667	6.18		2.42	3.76		0.052219

Test 38
Pipe: 18.5 mm
OCR: 5%
Apparent Superheat: 15°C
Mass Flux: 60 kg/m^2s

P_sat	OCR	T_ref_evap_out	T_ref_evap_wall
1208	0.0506	27.1	26.4

T_sat	T_ref_evap_in	T_w_e_in	T_w_e_out
13.7	9.0	27.2	24.9

T_ref_cond_out	T_ref_subcooler_out	T_oil
11.0	8.8	7.6

m_ref	m_oil	m_ref_oil	m_water
14.02	1.80	15.83	313

rho_ref	rho_oil	OMF oil tank
1135.3	1046.0	0.444

dP_refoil_h	dP_refoil_v	dp_refoil_evap
		2.14

dH_refoil	G_mass_flux
187.8	59.5

Weight Measurement Sheet							Tube weights (g)	
Date	3/25/2010						horizontal	2943.16
Tester	ankit						vertical	3004.12
Filename:	OMF5_x15_m16_Mar2510_1226							
	Sheath Weights full (g)			Final	Sheath weights vented			final
Horizonta	511.63	511.62	511.61	511.62	511.59	511.6	511.6	511.5967
Vertical	511.63	511.62	511.61	511.62	511.59	511.6	511.6	511.5967
	Sheath + Full Tube Weight (g)							
Horizonta	3508.72	3508.67	3508.73				3508.707	
Vertical	3615.61	3615.62	3615.55				3615.593	
	Sheath + Vented Tube Weight (g)							
Horizonta	3483.51	3483.49	3483.52				3483.507	
Vertical	3578.11	3578.14	3578.1				3578.117	
	Measured				Calculated			
	oil	R410a	sum		oil	R410a		error
Horizonta	28.75	25.17667	53.92667		27.51	26.41667		0.04313
Vertical	62.4	37.45333	99.85333		61.74	38.11333		0.010577

Test 39
Pipe: 18.5 mm
OCR: 5%
Apparent Superheat: 15°C
Mass Flux: 70 kg/m^2s

P_sat	OCR	T_ref_evap_out	T_ref_evap_wall
1221	0.0523	27.5	26.8

T_sat	T_ref_evap_in	T_w_e_in	T_w_e_out
14.1	8.4	27.8	25.1

T_ref_cond_out	T_ref_subcooler_out	T_oil
10.9	8.4	7.5

m_ref	m_oil	m_ref_oil	m_water
16.42	2.10	18.53	320

rho_ref	rho_oil	OMF oil tank
1137.3	1043.0	0.461

dP_refoil_h	dP_refoil_v	dp_refoil_evap
		2.92

dH_refoil	G_mass_flux
190.0	69.7

Weight Measurement Sheet

Date	3/23/2010
Tester	kurt and ankit

Tube weights (g)	
horizontal	2943.16
vertical	3004.12

Filename: OMF5_x15_m18_Mar2410_1148

	Sheath Weights full (g)			Final	Sheath weights vented			final
Horizonta	510.68	510.67	510.68	510.6767	510.86	510.88	510.84	510.86
Vertical	510.68	510.67	510.68	510.6767	510.86	510.88	510.84	510.86

	Sheath + Full Tube Weight (g)						
Horizonta	3505.2	3505.16	3505.15				3505.17
Vertical	3611.64	3611.65	3611.65				3611.647

	Sheath + Vented Tube Weight (g)						
Horizonta	3480.54	3480.59	3480.5				3480.543
Vertical	3575.12	3575.15	3575.08				3575.117

	Measured				Calculated			
	oil	R410a	sum		oil	R410a		error
Horizonta	26.5233333	24.81	51.33333		24.97	26.36333		0.058565
Vertical	60.1366667	36.71333	96.85		58.49	38.36		0.027382

Test 40
Pipe: 18.5 mm
OCR: 5%
Apparent Superheat: 15°C
Mass Flux: 70 kg/m^2s

P_sat	OCR	T_ref_evap_out	T_ref_evap_wall
1210	0.0505	26.7	26.2

T_sat	T_ref_evap_in	T_w_e_in	T_w_e_out
13.8	9.5	27.1	24.2

T_ref_cond_out	T_ref_subcooler_out	T_oil
10.9	9.6	8.7

m_ref	m_oil	m_ref_oil	m_water
16.57	2.16	18.73	290

rho_ref	rho_oil	OMF oil tank
1133.1	1044.4	0.439

dP_refoil_h	dP_refoil_v	dp_refoil_evap
		3.15

dH_refoil	G_mass_flux
188.7	70.4

Weight Measurement Sheet

Date: 4/13/2010
Tester: kurt

Tube weights (g)	
horizontal	2943.16
vertical	3004.12

Filename: OMF5_x15_m19_Apr1310_1114

	Sheath Weights full (g)			Final	Sheath weights vented			final
Horizonta	513.08	513.08		513.08	513.05	513.06	513.05	513.0533
Vertical	513.08	513.08		513.08	513.05	513.06	513.05	513.0533

	Sheath + Full Tube Weight (g)			
Horizonta	3507.57	3507.54	3507.53	3507.547
Vertical	3616.56	3616.59	3616.58	3616.577

	Sheath + Vented Tube Weight (g)			
Horizonta	3481.65	3481.65	3481.65	3481.65
Vertical	3580.07	3580.05	3580.04	3580.053

	Measured			Calculated		
	oil	R410a	sum	oil	R410a	error
Horizonta	25.4366667	25.87	51.30667	25.1	26.20667	0.013235
Vertical	62.88	36.49667	99.37667	60.6	38.77667	0.03626

Test 41
Pipe: 18.5 mm
OCR: 5%
Apparent Superheat: 15°C
Mass Flux: 70 kg/m^2s

P_sat	OCR	T_ref_evap_out	T_ref_evap_wall
1294	0.0500	31.1	30.1

T_sat	T_ref_evap_in	T_w_e_in	T_w_e_out
16.1	10.2	31.3	28.6

T_ref_cond_out	T_ref_subcooler_out	T_oil
13.5	10.1	9.5

m_ref	m_oil	m_ref_oil	m_water
16.58	2.03	18.61	308

rho_ref	rho_oil	OMF oil tank
1131.4	1038.7	0.458

dP_refoil_h	dP_refoil_v	dp_refoil_evap
		2.83

dH_refoil	G_mass_flux
190.5	70.0

Weight Measurement Sheet
Date: 4/14/2010
Tester: kurt and ankit

Tube weights (g)	
horizontal	2943.16
vertical	3004.12

Filename: OMF5_x15_m19_Apr1410_0954

	Sheath Weights full (g)			Final	Sheath weights vented			final
Horizonta	513.45	513.44	513.44	513.4433	513.43	513.45	513.4	513.4267
Vertical	513.45	513.44	513.44	513.4433	513.43	513.45	513.4	513.4267

	Sheath + Full Tube Weight (g)						
Horizonta	3510.47	3510.46	3510.49				3510.473
Vertical	3621.65	3621.66	3621.66				3621.657

	Sheath + Vented Tube Weight (g)						
Horizonta	3484.6	3484.6	3484.6				3484.6
Vertical	3583.4	3583.39	3583.39				3583.393

	Measured				Calculated			
	oil	R410a	sum		oil	R410a		error
Horizonta	28.0133333	25.85667	53.87		26.68	27.19		0.047596
Vertical	65.8466667	38.24667	104.0933		64.45	39.64333		0.021211

Test 42
Pipe: 18.5 mm
OCR: 5%
Apparent Superheat: 15°C
Mass Flux: 80 kg/m^{2}s

P_sat	OCR	T_ref_evap_out	T_ref_evap_wall
1278	0.0511	27.9	27.1

T_sat	T_ref_evap_in	T_w_e_in	T_w_e_out
15.7	8.6	28.6	25.6

T_ref_cond_out	T_ref_subcooler_out	T_oil
12.4	8.6	7.8

m_ref	m_oil	m_ref_oil	m_water
18.65	2.47	21.12	324

rho_ref	rho_oil	OMF oil tank
1136.7	1047.0	0.437

dP_refoil_h	dP_refoil_v	dp_refoil_evap
		3.66

dH_refoil	G_mass_flux
189.2	79.4

Weight Measurement Sheet						Tube weights (g)	
Date	3/23/2010					horizontal	2943.16
Tester	kurt and ankit					vertical	3004.12
Filename:	OMF5_x15_m21_Mar2310_1220						
	Sheath Weights full (g)			Final	Sheath weights vented		final
Horizonta	510.15	510.14	510.15	510.1467	510.18	510.19	510.18	510.1833
Vertical	510.15	510.14	510.15	510.1467	510.18	510.19	510.18	510.1833
	Sheath + Full Tube Weight (g)							
Horizonta	3503.2	3503.17	3503.19				3503.187	
Vertical	3598.8	3598.75	3598.8				3598.783	
	Sheath + Vented Tube Weight (g)							
Horizonta	3477.52	3477.51	3477.55				3477.527	
Vertical	3563.42	3563.4	3563.43				3563.417	
	Measured				Calculated			
	oil	R410a	sum		oil	R410a		error
Horizonta	24.1833333	25.69667	49.88		22.46	27.42		0.071261
Vertical	49.1133333	35.40333	84.51667		46.88	37.63667		0.045473

Test 43
Note: The saturation temperature drifted up to 15.7°C at this high mass flux due to system limitations.
Pipe: 18.5 mm
OCR: 5%
Apparent Superheat: 15°C
Mass Flux: 100 kg/m^{2}s

P_sat	OCR	T_ref_evap_out	T_ref_evap_wall
1279	0.0500	29.7	28.9

T_sat	T_ref_evap_in	T_w_e_in	T_w_e_out
15.7	8.7	30.5	26.8

T_ref_cond_out	T_ref_subcooler_out	T_oil
11.8	8.8	8.4

m_ref	m_oil	m_ref_oil	m_water
23.52	3.00	26.52	326

rho_ref	rho_oil	OMF oil tank
1136.7	1044.4	0.443

dP_refoil_h	dP_refoil_v	dp_refoil_evap
		6.79

dH_refoil	G_mass_flux
189.1	99.7

Weight Measurement Sheet

Date	4/2/2010
Tester	kurt and ankit

Tube weights (g)	
horizontal	2943.16
vertical	3004.12

Filename: OMF5_x15_m26_Apr0210_1612

	Sheath Weights full (g)			Final	Sheath weights vented			final
Horizonta	512.57	512.57	512.57	512.57				#DIV/0!
Vertical	512.57	512.57	512.57	512.57				#DIV/0!

	Sheath + Full Tube Weight (g)						
Horizonta	3501.17	3501.18	3501.19				3501.18
Vertical	3593.21	3593.21	3593.21				3593.21

	Sheath + Vented Tube Weight (g)						
Horizontal							#DIV/0!
Vertical							#DIV/0!

	Measured				Calculated			
	oil	R410a	sum		oil	R410a		error
Horizontal			45.45		19.91	25.54		
Vertical			76.52		42.35	34.17		

Test 44
Note: The saturation temperature drifted up to 16.1°C at this high mass flux due to system limitations.
Pipe: 18.5 mm
OCR: 5%
Apparent Superheat: 15°C
Mass Flux: 100 kg/m^2s

P_sat	OCR	T_ref_evap_out	T_ref_evap_wall
1293	0.0511	31.1	30.2

T_sat	T_ref_evap_in	T_w_e_in	T_w_e_out
16.1	9.0	31.6	28.0

T_ref_cond_out	T_ref_subcooler_out	T_oil
12.2	9.1	9.0

m_ref	m_oil	m_ref_oil	m_water
23.40	2.94	26.35	340

rho_ref	rho_oil	OMF oil tank
1135.9	1040.0	0.458

dP_refoil_h	dP_refoil_v	dp_refoil_evap
		6.39

dH_refoil	G_mass_flux
190.6	99.1

Weight Measurement Sheet
Date 4/12/2010
Tester Kurt andf Ankit

Tube weights (g)	
horizontal	2943.16
vertical	3004.12

Filename: OMF5_x15_m26_Apr1210_1110

	Sheath Weights full (g)			Final	Sheath weights vented			final
Horizonta	512.7	512.7	512.7	512.7	512.9	512.89	512.9	512.8967
Vertical	512.7	512.7	512.7	512.7	512.9	512.89	512.9	512.8967

	Sheath + Full Tube Weight (g)						
Horizonta	3505.17	3505.16	3505.16				3505.163
Vertical	3600.93	3600.98	3600.95				3600.953

	Sheath + Vented Tube Weight (g)						
Horizonta	3479.13	3479.14					3479.135
Vertical	3565.87	3565.87					3565.87

	Measured				Calculated			
	oil	R410a	sum		oil	R410a		error
Horizonta	23.0783333	26.225	49.30333		23.16	26.14333		0.003539
Vertical	48.8533333	35.28	84.13333		48.87	35.26333		0.000341

Test 45
Pipe: 18.5 mm
OCR: 3%
Apparent Superheat: 15°C
Mass Flux: 70 kg/m^{2}s

P_sat	OCR	T_ref_evap_out	T_ref_evap_wall
1178	0.0297	27.2	26.7

T_sat	T_ref_evap_in	T_w_e_in	T_w_e_out
12.8	8.4	27.5	24.7

T_ref_cond_out	T_ref_subcooler_out	T_oil
9.6	8.4	7.0

m_ref	m_oil	m_ref_oil	m_water
17.19	1.46	18.65	309

rho_ref	rho_oil	OMF oil tank
1137.3	1061.0	0.379

dP_refoil_h	dP_refoil_v	dp_refoil_evap
		3.38

dH_refoil	G_mass_flux
198.9	70.1

Weight Measurement Sheet
Date 3/30/2010
Tester kurt and ankit

Tube weights (g)	
horizontal	2943.16
vertical	3004.12

Filename: OMF3_x15_m19_Mar3010_1150

	Sheath Weights full (g)			Final	Sheath weights vented			final
Horizonta	511.2	511.2	511.2	511.2	511.21	511.24	511.22	511.2233
Vertical	511.2	511.2	511.2	511.2	511.21	511.24	511.22	511.2233

	Sheath + Full Tube Weight (g)			
Horizonta	3495.55	3495.55	3495.57	3495.557
Vertical	3600	3600.03	3600.09	3600.04

	Sheath + Vented Tube Weight (g)			
Horizonta	3472.3	3472.32	3472.3	3472.307
Vertical	3567.52	3567.47	3567.49	3567.493

	Measured			Calculated		
	oil	R410a	sum	oil	R410a	error
Horizonta	17.9233333	23.27333	41.19667	18.25	22.94667	0.018226
Vertical	52.15	32.57	84.72	51.21	33.51	0.018025

Test 46
Pipe: 18.5 mm
OCR: 3%
Apparent Superheat: 15°C
Mass Flux: 80 kg/m^{2}s

P_sat	OCR	T_ref_evap_out	T_ref_evap_wall
1279	0.0301	27.4	26.8

T_sat	T_ref_evap_in	T_w_e_in	T_w_e_out
15.7	7.9	28.7	25.4

T_ref_cond_out	T_ref_subcooler_out	T_oil
12.4	8.1	7.1

m_ref	m_oil	m_ref_oil	m_water
20.02	1.50	21.51	312

rho_ref	rho_oil	OMF oil tank
1139.7	1049.5	0.433

dP_refoil_h	dP_refoil_v	dp_refoil_evap
		4.05

dH_refoil	G_mass_flux
199.3	80.9

Weight Measurement Sheet
Date 3/29/2010
Tester kurt and ankit

Tube weights (g)	
horizontal	2943.16
vertical	3004.12

Filename: OMF3_x15_m21_Mar2910_1004

	Sheath Weights full (g)			Final	Sheath weights vented			final
Horizonta	510.8	510.8	510.8	510.8	510.88	510.87	510.87	510.8733
Vertical	510.8	510.8	510.8	510.8	510.88	510.87	510.87	510.8733

	Sheath + Full Tube Weight (g)						
Horizonta	3494.18	3494.23	3494.27				3494.227
Vertical	3583.17	3583.13	3583.16				3583.153

	Sheath + Vented Tube Weight (g)						
Horizonta	3470.66	3470.73	3470.66				3470.683
Vertical	3551.75	3551.75	3551.79				3551.763

	Measured				Calculated			
	oil	R410a	sum		oil	R410a		error
Horizonta	16.65	23.61667	40.26667		15.32	24.94667		0.07988
Vertical	36.77	31.46333	68.23333		34.81	33.42333		0.053304

Test 47
Pipe: 18.5 mm
OCR: 3%
Apparent Superheat: 15°C
Mass Flux: 100 kg/m^2s

P_sat	OCR	T_ref_evap_out	T_ref_evap_wall
1305	0.0298	29.3	28.7

T_sat	T_ref_evap_in	T_w_e_in	T_w_e_out
16.4	9.1	30.3	26.4

T_ref_cond_out	T_ref_subcooler_out	T_oil
12.5	9.3	8.8

m_ref	m_oil	m_ref_oil	m_water
24.75	1.64	26.39	319

rho_ref	rho_oil	OMF oil tank
1134.8	1036.6	0.478

dP_refoil_h	dP_refoil_v	dp_refoil_evap
		6.54

dH_refoil	G_mass_flux
198.5	99.3

Weight Measurement Sheet							Tube weights (g)	
Date	4/2/2010						horizontal	2943.16
Tester	kurt and ankit						vertical	3004.12
Filename:	OMF3_x15_m26_Apr0210_1138							
	Sheath Weights full (g)			Final	Sheath weights vented			final
Horizonta	512.58	512.59	512.6	512.59	512.69	512.65	512.6	512.6467
Vertical	512.58	512.59	512.6	512.59	512.69	512.65	512.6	512.6467
	Sheath + Full Tube Weight (g)							
Horizonta	3498.39	3498.4	3498.37				3498.387	
Vertical	3584.24	3584.23	3584.22				3584.23	
	Sheath + Vented Tube Weight (g)							
Horizonta	3472.5	3472.5	3472.48				3472.493	
Vertical	3550.69	3550.68	3550.68				3550.683	
	Measured				Calculated			
	oil	R410a	sum		oil	R410a		error
Horizonta	16.6866667	25.95	42.63667		17.03	25.60667		0.020575
Vertical	33.9166667	33.60333	67.52		34.34	33.18		0.012482

There was some difficulty with the oil entering the taps for the differential pressure transducers. It was observed that the oil only entered through the pressure taps during closing or opening of valves while the system was running. In order to eliminate errors in pressure drop measurements, the pressure drop measurements for the 18.5 mm pipe were taken all at once, without closing the valves at all in between test conditions. This provided pressure drop measurements with accurate values, which are shown below.

G	OCR	Δp_h	Δp_v
kg/m^{2}s		kPa	kPa
79.6	0.0321	0.36	1.88
70.9	0.0303	0.3	1.65
59.8	0.0315	0.23	1.52
50.7	0.0312	0.2	1.6
39.6	0.0306	0.12	2.6
29.9	0.0307	0.06	3.67
100.6	0.052	0.53	2.65
79	0.0529	0.36	2.53
69.8	0.0524	0.33	2.37
59.5	0.0501	0.23	2.01
50.2	0.049	0.19	2.05
40.5	0.0502	0.12	2.99
29.9	0.0512	0.09	4.75